

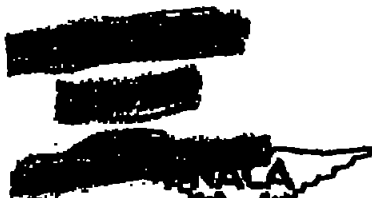
NATIONAL ADVISORY COMMITTEE FOR AERONAUTICS

TECHNICAL NOTE 4647

A STUDY OF THE MOTION AND AERODYNAMIC HEATING OF MISSILES ENTERING THE EARTH'S ATMOSPHERE AT HIGH SUPERSONIC SPEEDS

By H. Julian Allen and A. J. Eggers, Jr.

Ames Aerautical Laboratory
Moffett Field, Calif.



Washington
October 1967

NATIONAL ADVISORY COMMITTEE FOR AERONAUTICS

TECHNICAL NOTE 4647

A STUDY OF THE MOTION AND AERODYNAMIC HEATING OF MISSILES ENTERING THE EARTH'S ATMOSPHERE AT HIGH SUPERSONIC SPEEDS¹

By H. Julian Allen and A. J. Eggers, Jr.

SUMMARY

A simplified analysis is made of the velocity and deceleration history of missiles entering the earth's atmosphere at high supersonic speeds. It is found that, in general, the gravity force is negligible compared to the aerodynamic drag force and, hence, that the trajectory is essentially a straight line. A constant drag coefficient and an exponential variation of density with altitude are assumed and generalized curves for the variation of missile speed and deceleration with altitude are obtained. A curious finding is that the maximum deceleration is independent of physical characteristics of a missile (e.g., mass, size, and drag coefficient) and is determined only by entry speed and flight-path angle, provided this deceleration occurs before impact. This provision is satisfied by missiles presently of more usual interest.

The results of the motion analysis are employed to determine means available to the designer for minimizing aerodynamic heating. Emphasis is placed upon the convective-heating problem including not only the total heat transfer but also the maximum average and local rates of heat transfer per unit area. It is found that if a missile is so heavy as to be retarded only slightly by aerodynamic drag, i.e., irrespective of the magnitude of the drag force, then convective heating is minimized by minimizing the total shear force acting on the body. This condition is achieved by employing shapes with a low pressure drag. On the other hand, if a missile is so light as to be decelerated to relatively low speeds, even if acted upon by low drag forces, then convective heating is minimized by employing shapes with a high pressure drag, thereby maximizing the amount of heat delivered to the atmosphere and minimizing the amount delivered to the body in the deceleration process. Blunt shapes appear superior to slender shapes from the standpoint of having lower maximum convective heat-transfer rates in the region of the nose. The maximum average heat-transfer rate per unit area can be reduced by

¹Superseded recently declassified NACA R4 A53026 by H. Julian Allen and A. J. Eggers, Jr., 1973.

employing either slender or blunt shapes rather than shapes of intermediate slenderness. Generally, the blunt shape with high pressure drag would appear to offer considerable promise of minimizing the heat transfer to missiles of the sizes, weights, and speeds presently of interest.

INTRODUCTION

In the design of long-range rocket missiles of the ballistic type, one of the most difficult phases of flight the designer must cope with is the re-entry into the earth's atmosphere, wherein the aerodynamic heating associated with the high flight speeds of such missiles is intense. The air temperature in the boundary layer may reach values in the tens of thousands of degrees Fahrenheit which, combined with the high surface shear, promotes very great convective heat transfer to the surface. Heat-absorbent material must therefore be provided to prevent destruction of the essential elements of the missile. It is a characteristic of long-range rockets that for every pound of material which is carried to "burn-out," many pounds of fuel are required in the booster to obtain the flight range. It is clear, therefore, that the amount of material added to protect the warhead from excessive aerodynamic heating must be minimized in order to keep the take-off weight to a practicable value. The importance of reducing the heat transferred to the missile to the least amount is thus evident.

For missiles designed to absorb the heat within the solid surface of the missile shell, a factor which may be important, in addition to the total amount of heat transferred, is the rate at which it is transferred since there is a maximum rate at which the surface material can safely conduct the heat within itself. An excessively high time rate of heat input may promote such large temperature differences as to cause spalling of the surface, and thus result in loss of valuable heat-absorbent material, or even structural failure as a result of stresses induced by the temperature gradients.

For missiles designed to absorb the heat with liquid coolants (e.g., by "sweat cooling" where the surface heat-transfer rate is high, or by circulating liquid coolants within the shell where the surface heat-transfer rate is lower), the time rate of heat transfer is similarly of interest since it determines the required liquid pumping rate.

These heating problems, of course, have been given considerable study in connection with the design of particular missiles, but these studies are very detailed in scope. There has been need for a generalized heating analysis intended to show in the broad sense the means available for minimizing the heating problems. Wagner, reference 1,

made a step toward satisfying this need by developing a reasonably simple motion analysis. This analysis was not generalized, however, since it was his purpose to study the motion and heating of a particular missile.

It is the purpose of this report to simplify and generalize the analysis of the heating problem in order that the salient features of this problem will be made clear so that successful solutions of the problem will suggest themselves.

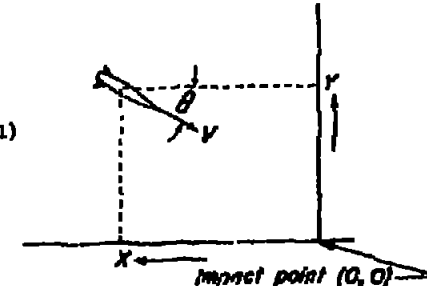
A motion analysis, having the basic character of Wagner's approach, precedes the heating analysis. The generalized results of this analysis are of considerable interest in themselves and, accordingly, are treated in detail.

ANALYSIS

Motion of the Body

Consider a body of mass m entering the atmosphere from great height. If, at any altitude y , the speed is V and the angle of approach is θ to the horizontal (see sketch), the parametric equations of motion can be written²

$$\left. \begin{aligned} \frac{dy}{dt^2} &= -g + \frac{C_D \rho V^2 A}{2m} \sin \theta \\ \frac{dx}{dt^2} &= \frac{C_D \rho V^2 A}{2m} \cos \theta \end{aligned} \right\} (1)$$



²Properly, the analysis should consider those effects resulting from the fact that the earth is a rotating sphere, but since the altitude range for which drag effects are important is less than 1 percent of the radius of the earth, the rectilinear treatment given in this analysis is permissible.

where

 C_D drag coefficient, dimensionless V speed, ft/sec A reference area for drag evaluation, sq ft m mass of the body, slugs ρ mass density of the air, slugs/ft³ g acceleration of gravity, ft/sec² x, y horizontal and vertical distance from the point of impact with the earth, ft θ angle between the flight path and the horizontal, deg

(See Appendix A for complete list of symbols.)

In general, the drag coefficient varies with Mach number and Reynolds number, while the density and, to a very minor extent, the acceleration of gravity vary with altitude. Hence it is clear that exact solution of these equations is formidable. Let us first, then, consider the following simplified case:

1. The body descends vertically.
2. The drag coefficient is constant.³
3. The acceleration of gravity is constant.⁴
4. The density as a function of altitude is given by the relation

$$\rho = \rho_0 e^{-By} \quad (2)$$

where ρ_0 and B are constants. This relation is consistent with the assumption of an isothermal atmosphere.

³As is well known, this assumption is generally of good accuracy at the high Mach numbers under consideration, at least as long as the total drag is largely pressure drag.

⁴The acceleration of gravity decreases by only 1 percent for every 100,000-foot increase in altitude.

Equations (1) then reduce to the single equation

$$\frac{d^2Y}{dt^2} = -\frac{dY}{dt} = -g + \frac{C_D \rho_0 A}{2m} e^{-By} V^2 \quad (3)$$

Noting that

$$\frac{dY}{dt} = -V \frac{dV}{dy}$$

we let

$$Z = V^2$$

and equation (3) becomes the linear differential equation

$$\frac{dZ}{dy} - \frac{C_D \rho_0 A}{m} e^{-By} Z + 2g = 0 \quad (4)$$

which has the well-known solution

$$Z = e^{\int \frac{C_D \rho_0 A}{m} e^{-By} dy} \left(-2g \int e^{-\int \frac{C_D \rho_0 A}{m} e^{-By} dy} dy + \text{const.} \right)$$

Performing the integrations, we obtain as the solution of this relation

$$Z = V^2 = e^{-\frac{C_D \rho_0 A}{m} e^{-By}} \left[\frac{2g}{B} \sum_{n=1}^{\infty} \frac{\left(\frac{C_D \rho_0 A}{m} e^{-By} \right)^n}{n!} - 2gy + \text{const.} \right] \quad (5)$$

so that the deceleration becomes, in terms of gravity acceleration,

$$-\frac{dV}{dt} = \frac{C_D \rho_0 A}{2mg} e^{-By} - \frac{C_D \rho_0 A}{m} e^{-By} \left[\frac{2g}{B} \sum_{n=1}^{\infty} \frac{\left(\frac{C_D \rho_0 A}{m} e^{-By} \right)^n}{n! n} - 2gy + \text{const.} \right]^{-1} \quad (6)$$

As an example, consider the vertical descent of a solid iron sphere having a diameter of 1 foot. For a sphere the drag coefficient may be taken as unity, based on the frontal area for all Mach numbers greater than about 1.4. In equation (2), which describes the variation of density with altitude, the constants should clearly be so chosen as to give accurate values of the density over the range of altitudes for which the deceleration is large. It is seen in figure 1 that for

$$\rho_0 = 0.0034 \text{ slugs/ft}^3$$

and

$$g = \frac{1}{22,000} \text{ ft}^{-1}$$

which yields

$$\rho = 0.0034 e^{-\frac{y}{22,000}} \quad (7)$$

The calculated density is in good agreement with the NACA standard atmosphere values obtained from references 2 and 3 for the altitude range from 20,000 to 180,000 feet. These relations have been used in calculating the velocity and deceleration of the sphere for various altitudes, assuming vertical entrance velocities of 10,000, 20,000, and 30,000 feet per second at 40 miles altitude which, for these cases, may be considered the "outer reach" of the atmosphere. The results of these calculations are presented as the solid curves in figures 2 and 3.

It is seen in figure 3 that for the high entrance speeds considered, the decelerations reach large values compared to the acceleration of gravity. This suggests that the gravity term in equation (3) may be neglected without seriously affecting the results.³ When this term is neglected the equation of motion becomes

$$-\frac{dy}{dt} = V \frac{dy}{dy} + \frac{C_D \rho_0 A}{2m} e^{-By} \quad (8)$$

³It is usual to neglect the gravity acceleration a priori (see e.g., refs. 1 and 4.)

Integration gives

$$\ln V = -\frac{C_D \rho_0 A}{2mg} e^{-By} + \text{const.}$$

or

$$V = \text{const.} \times e^{-\frac{C_D \rho_0 A}{2mg} e^{-By}}$$

At the altitude of 40 miles it can readily be shown that the term

$$\times \frac{C_D \rho_0 A}{2mg} e^{-By}$$

is very nearly unity so that the velocity may be written

$$V = V_E e^{-\frac{C_D \rho_0 A}{2mg} e^{-By}} \quad (9)$$

and

$$-\frac{dy}{dt} = \frac{C_D \rho_0 A V_E^2}{2mg} e^{-By} - \frac{C_D \rho_0 A}{mg} e^{-By} \quad (10)$$

where V_E is the entrance speed.

By use of equations (9) and (10) the vertical-decent speeds and decelerations for the 1-foot-diameter sphere previously considered have been calculated for the same entrance speeds. The results are shown as the dashed curves in figures 2 and 3. It is seen that these approximate calculations agree very well with those based on the more complete equation of motion (eq. (3)).

The above finding is important, for it indicates that in the general case, wherein the body enters the atmosphere at high speed at angle θ_E to the horizontal, the gravity term, provided θ_E is not

too small, may be neglected in equation (1) to yield

$$\left. \begin{aligned} \frac{dy}{dt^2} &= \frac{C_D \rho V^2 A \sin \theta_E}{2m} \\ \frac{d^2y}{dt^2} &= \frac{C_D \rho V^2 A \cos \theta_E}{2m} \end{aligned} \right\} \quad (11)$$

so that the flight path is essentially a straight line (i.e., $\theta = \theta_E$), and the resultant deceleration equation becomes

$$-\frac{dv}{dt} = \frac{C_D \rho V^2}{2m} \quad (12)$$

Now, again, if the density relation given by equation (2) is used and it is noted that

$$V = \frac{-\frac{dy}{dt}}{\sin \theta_E} \quad \text{or} \quad -\frac{dy}{dt} = V \sin \theta_E \frac{dy}{dy}$$

equation (12) becomes

$$\frac{dy}{V} = \frac{C_D \rho_A A}{2m \sin \theta_E} e^{-By} dy$$

which can be integrated to yield

$$V = V_E e^{-\frac{C_D \rho_A A}{2m \sin \theta_E} By} \quad (13)$$

and the deceleration is then

$$-\frac{dv}{dt} = \frac{C_D \rho_A A V_E^2}{2m g} e^{-By} e^{-\frac{C_D \rho_A A}{2m \sin \theta_E} By} \quad (14)$$

The altitude y_1 at which the maximum deceleration occurs is found from this relation to be

$$y_1 = \frac{1}{B} \ln \frac{C_D \rho_A A}{2m \sin \theta_E} \quad (15)$$

If y_1 is positive, the velocity V_1 (from eqs. (13) and (15)) at which the maximum deceleration occurs becomes

$$V_1 = V_E e^{-\frac{1}{B}} \approx 0.61 V_E \quad (16)$$

and the value of the maximum deceleration is

$$-\left(\frac{dv}{dt} \right)_{\max} = -\left(\frac{dy}{dt} \right)_1 = \frac{V_E^2 \sin \theta_E}{2m g} \quad (17)$$

If equations (13) and (14) are rewritten to make the altitude reference point y_1 rather than zero, then

$$V = V_E e^{-\frac{C_D \rho_A A}{2m \sin \theta_E} (y_1 + \Delta y)}$$

and

$$-\frac{dv}{dt} = \frac{C_D \rho_A A V_E^2}{2m g} e^{-B(y_1 + \Delta y)} = \frac{C_D \rho_A A}{2m \sin \theta_E} e^{-B(y_1 + \Delta y)}$$

respectively, where Δy is the change in altitude from y_1 . Substitution of equation (15) into these expressions can readily be shown to give

$$\frac{V_{\Delta y}}{V_E} = e^{-\frac{1}{B} e^{-By}} = F'(By)$$

and

$$\begin{aligned} \left(\frac{dy/dt}{g} \right)_{AV} &= e^{-Ry} e^{(1-e^{-Ry})} = r''(Ry) \\ \left(\frac{dy/dt}{g} \right)_1 & \end{aligned} \quad (19)$$

Equations (18) and (19) are generalized expressions for velocity and deceleration for bodies of constant drag coefficient and, together with equations (15) and (17), can be used to determine the variation of these quantities with altitude for specific cases. The dependence of $r'(Ry)$ and $r''(Ry)$ on Ry is shown in figure 4.

The maximum deceleration and the velocity for maximum deceleration as given by equations (17) and (16) apply only if the altitude y_1 , given by equation (15), is positive. Otherwise the maximum deceleration in flight occurs at sea level with the velocity (see eq. (13))

$$V = V_0 - \frac{C_D \rho_0 A}{2mg} \sin \theta_0 \quad (20)$$

and has the value

$$-\left(\frac{dy}{dt} \right)_{MAX} = -\left(\frac{dy}{dt} \right)_0 = \frac{C_D \rho_0 A V_0^2}{2mg} e^{-\frac{C_D \rho_0 A}{2mg} \sin \theta_0} \quad (21)$$

Heating of the Body

It was noted previously that for practicable rocket missiles, it is vital that the weight of the missile be kept to a minimum. The total heat transferred to a missile from the air must be absorbed by some "coolant" material. Since this material has a maximum allowable temperature, it follows that it can accept only a given amount of heat per unit weight. Hence, the total heat input to the missile must be kept at a minimum for minimum missile weight.

Often the coolant material is simply the shell of the missile and as such must provide the structural strength and rigidity for the missile as well. The strength of the structure is dictated, in part, by the stresses induced by temperature gradients within the shell. Since these temperature gradients are proportional to the time rate of heat input, the maximum time rate of heat input is important in missile design. The heating, of course, varies along the surface but, since the shell transmits heat along as well as through itself, the strength of the structure as a whole may be determined by the maximum value of the average heat-transfer rate over the surface. This is simply the maximum value of the time rate of heat input per unit area. On the other hand, the structural strength at local points on the surface may be determined primarily by the local rate of heat input. Hence, the maximum time rate of heat input per unit area at the surface element where the heat transfer is greatest may also be of importance in design.

If liquid cooling is employed, the maximum surface heat-transfer rates retain their significance but, now, in the sense that they dictate such requirements as maximum coolant pumping rate, or perhaps shell porosity as well in the case of sweat cooling. Whichever the case, in the analysis to follow, these elements of the heating problem will be treated:

1. The total heat input
2. The maximum time rate of average heat input per unit area
3. The maximum time rate of local heat input per unit area

Since it is the primary function of this report to study means available to the missile designer to minimize the heating problem, the analysis is simplified to facilitate comparison of the relative heating of one missile with respect to another - accurate determination of the absolute heating of individual missiles is not attempted. With this point in mind, the following assumptions, discussed in Appendix B, are made:

1. Convective heat transfer predominates (i.e., radiation effects are negligible).
2. Effects of gaseous imperfections may be neglected.
3. Shock-wave boundary-layer interaction may be neglected.
4. Reynolds' analogy is applicable.
5. The Prandtl number is unity.

Total heat input. - The time rate of convective heat transfer from the air to any element of surface of the body may be expressed by the well-known relation

$$\frac{dQ}{dt} = h_1 (T_r - T_w)_1 \quad (22)$$

where

K heat transferred per unit area, ft-lb/ft²

h convective heat-transfer coefficient, $\frac{\text{ft-lb}}{\text{ft}^2 \text{ sec}^0 \text{R}}$

T_r recovery temperature, °R

T_w temperature of the wall, °R

t time, sec

and the subscript 1 denotes local conditions at any element of the surface ∂S .

It is convenient in part of this analysis to determine the heating as a function of altitude. To this end, noting that

$$dt = \frac{dy}{V \sin \theta_x}$$

we see that equation (22) may be written

$$\frac{dy}{dy} = - \frac{h_1(T_r - T_w)_1}{V \sin \theta_x} \quad (23)$$

With the assumption that the Prandtl number is unity, the recovery temperature is

$$T_r = T_1 \left(1 + \frac{\gamma-1}{2} M_1^2 \right) = T_1 \left(1 + \frac{\gamma-1}{2} M^2 \right)$$

where

M Mach number at the altitude y , dimensionless

γ the ratio of specific heat at constant pressure to that at constant volume, C_p/C_v , dimensionless

T static temperature at the altitude y , °R

so that

$$(T_r - T_w)_1 = T - T_{w1} + \frac{\gamma-1}{2} M^2 T$$

It is seen that for large values of the Mach number, which is the case of principal interest, the third term is large compared to reasonably allowable values of $T - T_w$. It will therefore be assumed that $T - T_w$ is negligible⁶ to that

$$(T_r - T_w)_1 = \frac{\gamma-1}{2} M^2 T \quad (24)$$

Moreover, since

$$M^2 T = \frac{V^2}{(\gamma-1) C_p}$$

equation (24) may be written

$$(T_r - T_w)_1 = \frac{V^2}{2C_p} \quad (25)$$

Now the local heat-transfer coefficient h_1 is, by Reynolds' analogy, for the assumed Prandtl number of unity

$$h_1 = \frac{1}{2} C_{f1} C_{p1} \rho_1 V_1 \quad (26)$$

where C_{f1} is the local skin-friction coefficient based on conditions V_1 , V_1 , etc., just outside the boundary layer. Then, since $(T_r - T_w)_1$ is essentially constant over the entire surface S , the rate of total

⁶It should be noted that without this assumption, the heat-input determination would be greatly complicated since the changing wall temperature with altitude would have to be considered to obtain the heat input (see e.g., ref. 1). For high-speed missiles which maintain high speed during descent, the assumption is obviously permissible. Even for high-speed missiles which finally decelerate to low speeds, the assumption is generally still adequate since the total heat input is largely determined by the heat transfer during the high-speed portion of flight.

heat transfer with altitude becomes from equations (23) through (26)

$$\frac{dQ}{dy} = \int \frac{dy}{dy} dy = -\frac{1}{kC_p \sin \theta_E} \int_{y_1}^y C_F' C_p A_1 V_1 dy$$

where Q is the heat transferred to the whole surface S . This equation may be written

$$\frac{dQ}{dy} = -\frac{C_F' \rho v^2 S}{k \sin \theta_E} \quad (27)$$

wherein C_{F_1} is set equal to C_F and

$$C_F' = \frac{1}{S} \int_S C_F \left(\frac{\rho_1}{\rho} \right) \left(\frac{V_1}{V} \right) dS \quad (28)$$

The parameter C_F' is termed "the equivalent friction coefficient," and will be assumed constant,⁷ independent of altitude, again on the premise that relative rather than absolute heating is of interest. With equations (2) and (15), then, equation (27) is written

$$\frac{dQ}{dy} = -\frac{C_F' k \rho A_1 V_E^2}{k \sin \theta_E} e^{-ky} = -\frac{C_F' \rho_0 A}{k \sin \theta_E} e^{-ky} \quad (29)$$

Comparison of equation (29) with equation (14) shows that the altitude rate of heat transfer is directly proportional to the

⁷This assumption would appear poor at first glance since the Mach number and Reynolds number variations are so large. Analysis has indicated, however, that the effects of Mach number and Reynolds number variation are nearly compensating. The variation in C_F' for typical conical missiles was found to be, at most, about 70 percent from the maximum C_F' in the altitude range in which 80 percent of the heat is transferred.

desceleration, so that

$$\frac{dQ/dy}{dV/dt} = \frac{mg}{2 \sin \theta_E} \left(\frac{C_F' S}{C_D A} \right) \quad (30)$$

and therefore the maximum altitude rate of heat transfer occurs at the altitude y_1 (see eq. (15)) and is given by

$$\left(\frac{dQ}{dy} \right)_{\max} = \left(\frac{dQ}{dy} \right)_1 = -\frac{\rho V_E^2}{k} \left(\frac{C_F' S}{C_D A} \right) \quad (31)$$

It follows, of course, that the altitude rate of heat transfer varies with incremental change in altitude from y_1 in the same manner as deceleration, and thus, see eq. (19))

$$\frac{(dQ/dy)_{\Delta y}}{(dQ/dy)_1} = F^*(\Delta y) \quad (32)$$

The total heat input to the body at impact follows from equation (29) (integrating over the limits $0 \leq y \leq \infty$) and is

$$Q = \frac{1}{k} \left(\frac{C_F' S}{C_D A} \right) \rho_0^2 \left(1 - e^{-\frac{C_F' \rho_0 A}{k \sin \theta_E} y} \right) \quad (33)$$

The impact velocity, V_0 (the velocity of body at $y = 0$), is

$$V_0 = V_E + \frac{C_F' \rho_0 A}{k \sin \theta_E}$$

so that equation (33) may be written in the alternative form

$$Q = \frac{1}{k} \left(\frac{C_F' S}{C_D A} \right) (V_E^2 - V_0^2) \quad (34)$$

Maximum time rate of average heat input per unit area. - To determine the time rate of average heat transfer per unit area, equations (25), (26), and (28) with equation (22) may be shown to give

$$\frac{dH_{av}}{dt} = \frac{1}{4} C_T' \rho v^2 \quad (35)$$

which, together with equations (2) and (13), becomes at altitude y

$$\frac{dH_{av}}{dt} = \frac{C_T' \rho_0 V_E^2}{4} e^{-\beta y} = \frac{C_T' \rho_0 A}{4 \rho m \sin \theta_E} e^{-\beta y} \quad (36)$$

The maximum time rate of average heat transfer per unit area is found from this expression to be

$$\left(\frac{dH_{av}}{dt} \right)_{max} = \left(\frac{dH_{av}}{dt} \right)_s = \frac{1}{60} \left(\frac{C_T'}{C_p A} \right) \pi V_E^2 \sin \theta_E \quad (37)$$

and it occurs at the altitude

$$y_s = \frac{1}{\beta} \ln \left(\frac{\pi p_0 A}{2 \rho m \sin \theta_E} \right) \quad (38)$$

where the velocity is

$$V_s = V_E e^{-\frac{1}{\beta}} \approx 0.72 V_E \quad (39)$$

As with altitude rate of heat transfer, it can be shown that

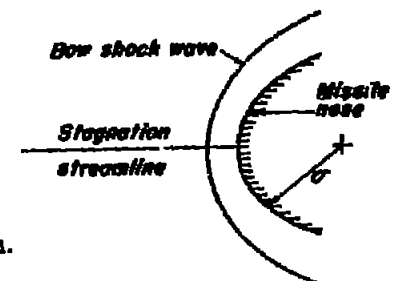
$$\frac{(dH_{av}/dt)_{dy}}{(dH_{av}/dt)_s} = r^2 (\Delta H) \quad (40)$$

Equations (37), (38), and (39) apply if the altitude for maximum time rate of average heat transfer per unit area occurs above sea level. If y_s , by equation (38), is negative, then this rate occurs at sea level and is, from equation (36),

$$\left(\frac{dH_{av}}{dt} \right)_{max} = \left(\frac{dH_{av}}{dt} \right)_0 = \frac{C_T' \rho_0 V_E^2}{4} e^{-\frac{C_T' \rho_0 A}{2 \rho m \sin \theta_E}} \quad (41)$$

Maximum time rate of local heat input per unit area. - The elemental surface which is subject to the greatest heat transfer per unit area is, except in unusual cases, the tip of the missile nose which first meets the air. It seems unlikely that a pointed nose will be of practical interest for high-speed missiles since not only is the local heat-transfer rate exceedingly large in this case, but the capacity for heat retention is small. Thus a truly pointed nose would burn away. Body shapes of interest for high-speed missiles would more probably, then, be those with nose shapes having nearly hemispherical tips. The following analysis applies at such tips.

It is well known that for any truly blunt body, the bow shock wave is detached and there exists a stagnation point at the nose. Consider conditions at this point and assume that the local radius of curvature of the body is σ (see sketch). The bow shock wave is normal to the stagnation streamline and converts the supersonic flow ahead of the shock to a low subsonic speed V_{st} at high static temperature T_{st} upstream of the shock. Thus, it is suggested that conditions near the stagnation point may be investigated by treating the nose section as if it were a segment of a sphere in a subsonic flow field.



The heat-transfer rate per unit area at the stagnation point is given by the relation

$$\frac{dH_{st}}{dt} = - \frac{\mu_{st} k_T (T_{st} - T_p)}{\sigma} \quad (42)$$

where k_T is the thermal conductivity of the gas at the recovery temperature (i.e., total temperature) T_r , and Re_T is the Reynolds number of the flow. If the flow is assumed to be laminar and incompressible,⁵ Re_T is given, according to reference 5, by the relationship

$$Re_T = 0.934 Re_0^{0.8} Pr^{2/3}$$

We retain the assumption that the Prandtl number is unity, note that $Re_0 = \rho v_0 / \mu_T$, and substitute equation (25) into equation (42) to obtain

$$\frac{dH_g}{dt} = 0.47 \sqrt{\frac{\rho k T}{\sigma}} v^2 \quad (43)$$

Now it is well known that at the high temperatures of interest here, the coefficient of viscosity μ_T varies nearly as the square root of the absolute temperature and is given by the relation

$$\mu_T = 2.31 \times 10^{-8} T_r^{1/2}$$

If this expression is combined with equation (25) (neglecting T_w), equation (43) may then be written⁶

$$\frac{dH_g}{dt} = 6.8 \times 10^{-6} \sqrt{\frac{\rho}{\sigma}} v^2 \quad (44)$$

⁵The assumption of constant density certainly may invalidate this analysis for any quantitative study of the relatively "cold-wall" flows of interest here. For the purpose of studying relative heat transfer it should, however, prove adequate.

⁶Cold wall conditions rather than recovery conditions been used in the development of equation (44), the relation

$$\frac{dH_g}{dt} = 1.1 \times 10^{-7} \sqrt{\frac{\rho}{\sigma}} v^2$$

would have been obtained assuming a linear variation of viscosity with temperature (to be consistent with the assumption of a cool wall). This relation would give somewhat higher heat-transfer rates per unit area than equation (44) at velocities greater than about 600 feet per second.

which, when combined with equations (2) and (13), becomes

$$\frac{dH_g}{dt} = 6.8 \times 10^{-6} \sqrt{\frac{\rho}{\sigma}} v_E^{1.8} e^{-\frac{3C_D A}{2\rho v} \sin \theta_E} \cdot e^{-Ry} \quad (45)$$

The maximum value of dH_g/dt can readily be shown to be

$$\left(\frac{dH_g}{dt} \right)_{\max} = \left(\frac{dH_g}{dt} \right)_0 = 6.8 \times 10^{-6} \sqrt{\frac{\rho v \sin \theta_E}{3C_D A}} v_E^3 \quad (46)$$

which occurs at the altitude

$$z_0 = \frac{1}{g} \ln \left(\frac{3C_D A}{\rho v \sin \theta_E} \right) \quad (47)$$

corresponding to the velocity

$$v_0 = v_E e^{-\frac{3C_D A}{2\rho v} \sin \theta_E} \approx 0.87 v_E \quad (48)$$

The manner in which the heat-transfer rate per unit area at the stagnation point varies with incremental change in altitude from y_0 can be shown to be

$$\frac{(dH_g/dt)_{\Delta z}}{(dH_g/dt)_0} = e^{-\frac{3C_D A}{2\rho v} \frac{1}{g} \left(-z - RY \right)} = F'''(RY) \quad (49)$$

The dependence of $F'''(RY)$ on RY is shown in Figure 1.

Equation (46) applies only if y_0 is above sea level. If y_0 , from equation (47), is negative, then the maximum heat-transfer rate per unit area at the stagnation point occurs at sea level and is

$$\left(\frac{dH_g}{dt} \right)_{\max} = \left(\frac{dH_g}{dt} \right)_0 = 4.9 \times 10^{-6} \sqrt{\frac{\rho}{\sigma}} v_E^{1.8} e^{-\frac{3C_D A}{2\rho v} \sin \theta_E} \quad (50)$$

DISCUSSION

Motion

The motion study shows some important features about the high-speed descent of missiles through the atmosphere. The major assumptions of this analysis were that the drag coefficient was constant and the density varied exponentially with altitude. It was found that the deceleration due to drag was generally large compared to the acceleration of gravity and, consequently, that the acceleration of gravity could be neglected in the differential equations of motion. The flight path was then seen to be a straight line, the missile maintaining the flight-path angle it had at entry to the atmosphere.

For missiles presently of more usual interest, the maximum deceleration occurs at altitude. One of the most interesting features of the flight of such a missile is that the maximum deceleration is independent of physical characteristics (such as mass, size, and drag coefficient of the missile), being dependent only on the entry speed and flight-path angle (see eq. (17)). The missile speed at maximum deceleration (eq. (16)) bears a fixed relation to the entrance speed (61 percent of entrance speed), while the corresponding altitude (eq. (15)) depends on the physical characteristics and the flight-path angle but not on the entrance speed. It is also notable that for a given incremental change in altitude from the altitude for maximum deceleration, the deceleration and speed bear fixed ratios to the maximum deceleration and the entry speed, respectively (see fig. 4 and eqs. (19) and (18)), hence, the deceleration and speed variation with altitude can readily be determined.

If the missile is very heavy, the calculated altitude for maximum deceleration (eq. (15)) may be fictitious (i.e., this altitude is negative) so the maximum deceleration is flight, which occurs just before impact at sea level, is less than that calculated by equation (17) and is dependent on the body characteristics as well as the entry speed and flight-path angle (see eq. (21)). However, the variation of speed and deceleration with altitude from the fictitious altitude given by equation (15) can still be obtained from figure 4.

Heating

Total heat input.— In the heating analysis, a number of simplifying assumptions were made which should limit its applicability to the determination of relative values of heating at hypersonic speeds. It is in this relative sense that the following discussion pertains.

In considering the total heat transferred by convection to a missile, it is evident from equation (33) that the course the designer should take to obtain the least heating is affected by the value of the factor

$$\frac{C_D \rho A}{\rho g \sin \theta_E} = B \quad (31)$$

To illustrate, first consider the case of a "relatively heavy" missile for which this factor is small compared to unity (the term "relatively heavy" is used to denote that the denominator involving the mass is very large as compared to the numerator involving the drag per unit dynamic pressure, $C_D A$). Then

$$1 - e^{-\frac{C_D \rho A}{\rho g \sin \theta_E}} \approx \frac{C_D \rho A}{\rho g \sin \theta_E}$$

is small compared to 1. If this function is expanded in series and only the leading term retained, equation (33) becomes

$$Q = \frac{C_f' \rho n V_E^2}{4 \rho \sin \theta_E} \quad (32)$$

For the relatively heavy missile, then, the least heat will be transferred when $C_f' S$ is a minimum—that is to say, when the total shear force acting on the body is a minimum. This result is as would be expected, if one notes that requiring $B \ll 1$ is tantamount to requiring the missile to be so heavy that it is retarded only slightly by aerodynamic drag in its motion through the atmosphere. Hence, the heat input to the missile is simply proportional to the shear force.

Now let us consider the case when $B \gg 1$, or, in other words, when this missile is "relatively light." In this event,

$$1 - e^{-\frac{C_D \rho A}{\rho g \sin \theta_E}} \approx 1$$

and equation (31) can be approximated

$$Q \approx \frac{1}{4} \rho n V_E^2 \left(\frac{C_f' S}{C_D A} \right)$$

For the relatively light missiles, then, the least convective heating is obtained when $C_f'B/C_pA$ is a minimum. This is at first glance a rather surprising result, for it indicates that the heating is reduced by increasing the total drag, provided the equivalent frictional drag is not increased proportionately as fast. Physically, this anomaly is resolved if the problem is viewed in the following way: The missile entering the atmosphere has the kinetic energy $1/2 m v_0^2$, but, if

$$\frac{C_p A y A}{m \sin \theta_E} = \left(\frac{v_0}{v_E} \right)^2$$

is small, then nearly all its entrance kinetic energy is lost, due to the action of aerodynamic forces, and must appear as heating of both the atmosphere and the missile. The fraction of the total heat which is given to the missile is,¹⁰ from equation (33),

$$\frac{1}{P} \left(\frac{T_E}{C_p} \right)$$

Thus, by keeping this ratio a minimum, as much as possible of the energy is given to the atmosphere and the missile heating is therefore least.

In order to illustrate these considerations in greater detail, calculations have been made using the previously developed equations to determine the heat transferred by convection to the air for several missiles. Two classes of missiles have been considered. Missiles in the first class were required to have a base area of 11 square feet. Missiles in the second class were required to have a base area of 1 square foot. Gross weights of 1, 1,000, 3,000, 10,000, and 20,000 pounds have been assumed, and the entrance angle, θ_E , has been taken as 1° in all cases. Missile heating, v_F to the air, has been calculated as a function of cone angle for entrance speeds of 1,000, 2,000, 3,000, and 5,000 feet per second. In calculating the friction-drag coefficient it was taken as constant for a particular value, the value corresponding to the entrance Mac number (a value of 1.5 was assumed throughout). These coefficients were determined for cones of 1°, 2°, 3°, 4°, 5°, 6°, 7°, 8°, 9°, 10°, 11°, 12°, 13°, 14°, 15°, 16°, 17°, 18°, 19°, and 20° cone angles of 10° and greater. For cone angles greater than 1°, reference 7 was employed to determine the friction-drag

¹⁰Note that even if all the drag is frictional, still, only half the heat is transferred to the body. The other half is transferred in the boundary layer and is left in the air by the δ_T .

(base drag was neglected in all cases). The total drag coefficient was taken as the sum of the pressure drag coefficient plus the skin-friction coefficient, the latter coefficient being taken at its value for maximum total heat-input rate with altitude. The boundary layer was assumed to be wholly turbulent since the Reynolds number, based on length of run along the surface of a cone and local conditions just outside the boundary layer, was always greater than about 6×10^5 and, in fact, was of the order of billions for the more slender cones. Turbulent-boundary-layer data were obtained from references 8 and 9, and Sutherland's law for the variation of viscosity with temperature was used in obtaining "equivalent flat-plate" heat-transfer x coefficients.

Missile heating calculated in this manner for the fixed-base-area and fixed-volume cones is presented in figures 5 and 6, respectively. Curves for missiles having densities greater than steel are considered improbable and are shown as dashed lines. It is clear that for both classes of bodies, when the missile is relatively heavy, the optimum solution is obtained by making $C_f'B$ as small as possible (small cone angle case) and this optimum is accentuated with increase in speed. On the other hand, when the missile is relatively light, reduced heating is obtained by making $C_f'B/C_pA$ as small as possible (the large cone angle case). It is noted also that, in general, the advantage of reduced heating of the relatively light, blunt cones is more pronounced in the fixed-base-area case than in the fixed-volume case.

Maximum time rate of average heat input per unit area.—It was previously noted that the maximum time rate of average heat input per unit area may be of serious importance in determining the structural integrity of missiles entering the atmosphere at high speeds.¹¹ In order to illustrate this fact, consider the case of a missile having a shell made of solid material and assume that the rate of heat transfer per unit area does not vary rapidly from one surface element to the next. Then the rate of transfer of heat along the shell will be small compared with the rate of transfer through the shell. The shell stress due to heat transfer is that resulting from the tendency toward differential expansion through the shell and it is proportional to $dT/d\eta$, where T_η is the temperature at any point η within the shell and η is measured perpendicular from the shell surface. We define k_s as the thermal conductivity of the shell material; then the rate at which heat transfers through the shell per unit area is $k_s(dT/d\eta)$ and this must, at $\eta = 0$, equal the rate of heat input per unit surface area. For the missile considered as a whole, the maximum value of the average thermal stress in the shell is a measure of the over-all structural

¹¹This is the common case when the shell material acts as structural support and must also transport or absorb the heat.

integrity and the maximum value of this stress will occur at the surface when

$$\frac{d\sigma_{av}}{ds} = \frac{1}{2} \left(\frac{d\sigma}{ds} \right)$$

is a minimum.

The course the designer should take to minimize the thermal stresses for the missile as a whole is dependent, as for the case of total heat input, upon whether the missile is relatively heavy or light. For the relatively heavy missile the value of β , given by equation (32), is small compared to unity. The maximum value of the average thermal stress in this case is proportional to (see eq. (41))

$$\left(\frac{\sigma_{av}}{s} \right) = \frac{C_p' \rho_0 V^2}{4} \quad (54)$$

and, hence, the least average thermal stress is obtained by making C_p' a minimum. On the other hand, for the relatively light missile the maximum value of the average thermal stress is proportional to (see eq. (37))

$$\left(\frac{\sigma_{av}}{s} \right) = \left(\frac{C_p'}{C_p A} \right) \frac{4 \pi V^2 \sin \theta_2}{6s} \quad (55)$$

and, hence, the least average thermal stress occurs when C_p'/A is a minimum.

In order to illustrate these considerations in greater detail, the maximum values of the time rate of average heat input per unit area have been calculated for the constant-base-area and the constant-volume cases previously discussed in the section on total heat input. These values were determined in much the same manner as those of total heat input, with the exception that C_p' was evaluated at y_2 (rather than y_1), given by equation (36) when it applies, and otherwise at $y_2 = 0$. The results are shown in figures 7 and 8. It is seen that the maximum values of average thermal stresses are reduced for both the slender cones and blunt cones as compared to the relatively large values of this stress experienced by cones of intermediate slenderness.

Maximum time rate of local heat input per unit area. - Perhaps even more important than the maximum value of the average shell stress is the maximum stress that occurs in the shell at the surface element of

the missile nose,¹² where the local heat-transfer rate is probably the greatest, for, in general, this latter stream is many times larger. In fact, this rate of local heat input can be so large as to produce temperature gradients through the shell that are intolerable even with the most highly conductive materials (copper, silver, etc.).¹³ Thus some additional means of cooling, such as sheet cooling, may, in any case, be required in this region.

It was stated previously that pointed-nose bodies are undesirable due, in part, to the fact that the local heat-transfer rate per unit area at the tip is excessive. The validity of this statement is demonstrated by the results of the analysis. It is clear (see eq. (44)) that since the local transfer rate varies inversely with the square root of the tip radius, not only should pointed bodies be avoided, but the rounded nose should have as large a radius as possible. The quantity then arises; if the nose radius is arbitrarily fixed, what source is available to the missile designer to minimize the problem of local heating at the stagnation point? From both equations (46) and (50), it is seen that for an arbitrary nose radius, if the mass, entry speed, and flight-path-angle are fixed, then the only way to reduce the stagnation rate of heat input per unit area is to increase the product $C_p A$. In fact, a relative stagnation-point heat-transfer rate per unit area, ψ , may be expressed in terms of B (see eq. (31)), if it is defined as the ratio of the maximum stagnation-point heat-transfer rate per unit area for a given missile to the maximum rate the same missile would experience if it were infinitely heavy. For the infinitely heavy missile, the maximum rate occurs at sea level and is (see eq. (50))

$$6.8 \times 10^{-4} \sqrt{\frac{\rho_0}{\sigma}} V^2$$

so that from equation (30)

$$\frac{C_p' \rho A}{B \rho_0 \sin \theta_2} = \frac{6.8}{\sqrt{\sigma}} \quad (56)$$

¹²In this report we are concerned only with bodies. If wings or stabilizers are used, their leading edges are similarly surface elements which experience intense heat transfer. The heating problem with wings and stabilizers is, in fact, so serious at very high speeds that their use as lifting surfaces appears, at present, inadmissible.

¹³See reference 1 for further discussion.

If the given missile also attains its maximum rate at sea level (i.e., $y_0 = 0$) eq. (47); whereas

$$\frac{1}{\rho} = \sqrt{\frac{\mu \sin \theta_0}{3c_D C_D^2 A}} = \frac{1}{\sqrt{3c_D}}$$
 (47)

If the given missile attains its maximum rate above sea level (eq. (46), y_0 positive). The variation of $\frac{1}{\rho}$ with $1/y_0$ is shown in figure 9. Clearly, the high pressure drag shape has the advantage over the slender shape in this respect.

In order to illustrate these considerations in greater detail, again consider the constant-base-area and constant-volume cones discussed earlier. Assume the pointed tips of all the cones are replaced by spherical tips of the same radius a . The relative effect of varying the cone angle on the stagnation-point heating can then be assessed by determining the variation of the product

$$\sqrt{a} \left(\frac{dR_p}{dt} \right)_{\text{max}}$$

This product has been calculated for the various cones, assuming C_D to be unaffected by the addition of the hemispherical tip (the tip radius may be arbitrarily small), and the results are shown in figures 10 and 11. It is seen again that the missiles having large cone angle (high drag coefficient) are considerably superior.

DESIGN CONSIDERATIONS AND CONCLUDING REMARKS

In the foregoing analysis and discussion, two aspects of the heating problem for missiles entering the atmosphere were treated. The first concerned the total heat absorbed by the missile and was related to the coolant required to prevent its disintegration. It was found that if a missile were relatively light, the least required weight of coolant (and hence of missile) is obtained with a shape having a high pressure drag coefficient, that is to say, a blunt shape. On the other hand, it was found that if the missile were relatively heavy the least required weight of coolant, and hence of missile, is obtained with a shape having a low skin-friction drag coefficient, that is to say, a long slender shape.

The second aspect of the heating problem treated was concerned with the rate of heat input, particularly with regard to thermal shell

stresses resulting therefrom. It was seen that the maximum average heat-input rate and, hence, maximum average thermal stress could be decreased by using either a blunt or a slender missile, while missiles of intermediate slenderness were definitely to be avoided in this connection. The region of highest local heat-transfer rate and, hence, probably greatest thermal stress was recorded to be located at the forward tip of the missile in most cases. This was assumed to be the case and it was found that the magnitude of this stress was reduced by employing a shape having the largest permissible tip radius and the smallest drag coefficient; that is to say, the blunt, high drag shape always appears to have the advantage in this respect.

The results provide us with rather "true," but useful, bases for designing shapes of missiles entering the atmosphere which have minimum heat-transfer problems. If, however, design considerations and tonnage, et al., dictate that the reentry missile be relatively heavy in the sense of eq. (46), that it must be most desirable that this missile have the blunt, especially if the entry speed is (say) 12,000 ft per sec. (entry). Despite the slender conical approximation to the actual shape of the vehicle, too, that the missile be made as blunt as possible will result in a lower radius to minimize the surface area, which in turn will reduce local shell stress problems. This is in contrast to the ordinary, slender, missile which has a relatively sharp nose and, hence, tends to generate a high heat flux at the nose (and cooling).

On the other hand, if the entry conditions are such that the missile must be relatively light, then the radius of the nose is believed to be of little importance in one respect, that is, giving a somewhat rounded nose, and a relatively large nose radius will result in a smaller surface area with these of course, the result being that the missile will be more efficient.

- spe velocity, resulting in a smaller surface area per unit volume.
- the nose radius is believed to be of little importance in one respect, that is, giving a somewhat rounded nose, and a relatively large nose radius will result in a smaller surface area.
- the nose radius, if relatively large, significantly assists in reducing the heat flux at the nose of the shell.

3. Aerodynamic forces are not sensitive to attitude and, hence, a sphere may need no stabilizing surfaces.
6. Because of this insensitivity to attitude, a sphere may possibly be rotated slowly, and perhaps even randomly,¹⁴ during flight, in order to subject all surface elements to about the same amount of heating and thereby approach uniform shell heating.

On the other hand, the sphere, in common with other very high drag shapes may be unacceptable if:

1. The low terminal speed permits effective countermeasures.
2. The lower average speed of descent increases the wind drift error at the target.
3. The magnitude of the maximum deceleration is greater than can be allowed.

The first two of these disadvantages of the sphere might be minimized by protruding a flow-separation-inducing spike from the front of the sphere to reduce the drag coefficient to roughly half (see ref. 11). Stabilization would now be required but only to the extent required to counterbalance the moment produced by the spike. Special provision would have to be made for cooling the spike.

These possible disadvantages of very high drag shapes may also be alleviated by another means, namely, using variable geometry arrangements. For example, an arrangement which suggests itself is a rounded shape with conical afterbody of low apex angle employing an extensible skirt at the base. With the skirt flared, the advantages of high drag are obtained during the entry phase of flight. As the air density increases with decreasing altitude, the skirt flare is decreased to vary the drag so as to produce the desired deceleration and speed history. If the deceleration is specified in the equation of motion (see motion analysis), the required variation of drag coefficient with altitude can be calculated and, in turn, the heating characteristics can be obtained.

¹⁴Note that if rotation is permitted, slow, random motion, may be required in order to prevent negative forces from causing deviation of the flight path from the target. It should also be noted that at subsonic and low supersonic speeds gun-fired spheres, presumably not rotating, have shown rather large lateral motions in flight (see ref. 10). It is not known whether such behavior occurs at high supersonic speeds.

The examples considered, of course, are included only to demonstrate some of the means the designer has at hand to control and diminish the aerodynamic heating problem. For simplicity, this problem has been treated, for the most part, in a relative rather than absolute fashion. In any final design, there is, of course, no substitute for step-by-step or other more accurate calculation of both the motion and aerodynamic heating of a missile.

Even from a qualitative point of view, a further word of caution must be given concerning the analysis of this paper. In particular, throughout, we have neglected effects of gaseous imperfections (such as dissociation) and shock-wave boundary-layer interaction on convective heat transfer to a missile, and of radiative heat transfer to or from the missile. One would not anticipate that these phenomena would significantly alter the conclusions reached on the relative merits of slender and blunt shapes from the standpoint of heat transfer at extreme speeds at least up to about 10,000 feet per second. It cannot tacitly be assumed, however, that this will be the case at higher entrance speeds (see Appendix B). Accurate conclusions regarding the dependence of heat transfer on shape for missiles entering the atmosphere at extremely high supersonic speeds must await the availability of more reliable data on the static and dynamic properties of air at the high temperatures and pressures that will be encountered.

Ames Aeronautical Laboratory
National Advisory Committee for Aeronautics
Moffett Field, Calif., Apr. 26, 1953

NACA TM 1047

APPENDIX A

SYMBOLS

A_0	reference area for drag evaluation, ft^2
B	body factor, dimensionless (See eq. (21).)
C_D	drag coefficient, dimensionless
C_f	skin-friction coefficient based on conditions just outside the boundary layer, dimensionless
$C_{f\bar{v}}$	equivalent skin-friction coefficient, dimensionless (See eq. (26).)
C_p	specific heat at constant pressure, $\frac{\text{ft-lb}}{\text{slug} \cdot ^\circ\text{R}}$
C_v	specific heat at constant volume, $\frac{\text{ft-lb}}{\text{slug} \cdot ^\circ\text{R}}$
F' , F'' , F'''	functions of $\frac{Re}{R}$, dimensionless (See eqs. (18), (19), and (45).)
g	acceleration due to force of gravity, $(\text{diam.})^{-2} \cdot 3.2 \cdot \frac{\text{ft}}{\text{sec}^2}$
h	convective heat-transfer coefficient, $\frac{\text{ft}-1}{\text{hr} \cdot ^\circ\text{R}}$
H	heat transferred per unit area, $\frac{\text{ft-lb}}{\text{hr}}$
k	thermal conductivity, $\frac{\text{ft-lb}}{\text{sec} \cdot \text{ft}^2 (\text{deg}/\text{ft})}$
m	mass, slugs
N	local number, dimensionless
Nu	Nusselt number, dimensionless

NACA TM 1047

31

Pr	Prandtl number, dimensionless
Q	total heat transferred, ft-lb
Re	Reynolds number, dimensionless
s	surface area, ft^2
T	temperature (ambient temperature of air at altitude y unless otherwise specified), $^\circ\text{R}$
t	time, sec
v	velocity, $\frac{\text{ft}}{\text{sec}}$
x, y	horizontal and vertical distance from impact point, ft
ξ	variable of integration, $\frac{\text{ft}^2}{\text{sec}^2}$
ρ	constant in density - altitude relation, ft^{-1} (See eq. (2)).
γ	ratio of specific heat at constant pressure to specific heat at constant volume, C_p/C_v , dimensionless
Δ	increment
δ	distance within the shell measured normal to shell surface, ft
θ	angle of flight path with respect to horizontal, deg
μ	coefficient of absolute viscosity, $\frac{\text{slugs}}{\text{ft sec}}$
ρ	air density, $\frac{\text{slug}}{\text{ft}^3}$
r	radius, ft
τ	relative heat-transfer factor, dimensionless (See eqs. (26) and (37).)

Subscripts

- o conditions at sea level ($y = 0$)
 z conditions at altitude y [eq. (15)]

conditions at altitude y_s (eq. (39))
 conditions at altitude y_s (eq. (47))
 conditions at entrance to earth's atmosphere
 local conditions
 recovery conditions
 stagnation conditions
 wall conditions
 conditions within the shell of the missile

APPENDIX B SIMPLIFYING ASSUMPTIONS IN THE CALCULATION OF AERODYNAMIC HEATING

As noted in the main body of the report, the heating analysis is simplified by making the following assumptions:

1. Convective heat transfer is of foremost importance; that is, radiative effects may be neglected.
2. Effects of gaseous imperfections, in particular dissociation, may be neglected.
3. Effects of shock-wave boundary-layer interaction may be neglected.
4. Reynolds' analogy is applicable.
5. Prandtl number is unity.

The restrictions imposed by these assumptions will now be considered in some detail.

In assumption 1, two simplifications are involved; namely, (1) radiation from the surface of the body is neglected, and (2) radiation to the body from the high-temperature disturbed air between the shock wave and the surface is neglected. The first simplification may be justified on the premise that the maximum allowable surface temperature will be about the same for one body as compared with another, irrespective of shape, and, consequently, radiation away from the surface will be approximately the same. Hence, neglecting this form of heat transfer should not appreciably change the relative heating which is of principal interest in this paper.

The second simplification of ignoring radiative heat transfer from the disturbed air to the body is not so easily treated. At ordinary flight speeds this form of heat transfer is negligible since it is well established that at temperatures not too different from ambient temperature, air is both a poor radiator and a poor absorber. At the flight speeds of interest, temperatures in the tens of thousands of degrees Fahrenheit may be easily obtained in the disturbed air flow, especially about the heavier blunt bodies. At these temperatures it does not follow, *a priori*, that air is a poor radiator. Data on the properties of air at these temperatures are indeed meager. Hence, it is clear that calculations of radiative heat transfer from air under

these conditions must, at best, be qualitative. Nevertheless, several such calculations have been made, assuming for lack of better information that air behaves as a grey body radiator and that Wein's law may be used to relate the wave length at which the maximum amount of radiation is emitted to the temperature of the air (this assumption, in effect, enables low-temperature data on the emissivity of air to be used in calculating radiation at high temperatures). In these calculations effects of dissociation in reducing the temperature of the disturbed air have also been neglected and hence from this standpoint, at least, conservative (i.e., too high) estimates of radiative heat transfer should evolve. The results of these calculations indicate the following: (1) Radiative heat transfer from the disturbed air to the body is of negligible importance compared to convective heat transfer at entrance speeds in the neighborhood of, or less than, 10,000 feet per second; (2) Radiative heat transfer, in the case of relatively massive blunt bodies, may have to be considered in heat-transfer calculations at entrance speeds in the neighborhood of 20,000 feet per second; (3) Radiative heat transfer, in the case of relatively massive blunt bodies, may be of comparable importance to convective heat transfer at entrance speeds in the neighborhood of 30,000 feet per second. From these results, we conclude, then, that the neglect of radiative heat transfer from the disturbed air to the body is probably permissible for all except, perhaps, very blunt and heavy shapes at entrance speeds up to 20,000 feet per second. However, this simplification may not be permissible, especially in the case of heavy blunt bodies entering the atmosphere at speeds in the neighborhood of, or greater than, 30,000 feet per second.

In assumption 2, the neglect of effects of gaseous imperfections, particularly dissociation, on convective heat transfer would appear to be permissible at entrance speeds up to and in the neighborhood of 10,000 feet per second, since at such speeds the temperatures of the disturbed air are not high enough for these imperfections to become significantly manifest. On the other hand, as the entrance speeds approach 20,000 feet per second, temperatures of the disturbed air may easily exceed 10,000° Rankine, in which case appreciable dissociation may be anticipated, inside the boundary layer for all bodies, and inside and outside the boundary layer in the case of blunt bodies. The magnitude of these effects is at present in some doubt (see, e.g., the results of refs. 12 and 13.) Hence, for the present, the neglect of effects of gaseous imperfections on convective heat transfer is not demonstrably permissible at entrance speeds in the neighborhood of 20,000 feet per second or greater.

In assumption 3, it has been shown by Lees and Probstein (ref. 14),

numbers in excess of about 10. Lees and Probstein found somewhat the opposite effect on heat-transfer rate in the case of weak interaction. It is not now known how this phenomenon depends upon body shape or type of boundary layer. However, it is reasonable to anticipate that there will be some effect, and certainly if the skin-friction coefficient is increased in order of magnitude at Mach numbers approaching 20, as indicated by the results of Li and Nagamatsu for strong interaction, then the phenomenon cannot be presumed negligible. Hence, we conclude that from this standpoint, also, the convective heat-transfer calculations of this report may be in error at entrance speeds of the order of 20,000 feet per second or greater.

The assumption that Reynolds' analogy may be used to relate skin-friction and heat-transfer coefficient does not, especially in the light of recent work by Rubesin (ref. 16), seem out of line with the purposes of this paper, at least at entrance speeds up to and in the neighborhood of 10,000 feet per second. However, it does not follow, *a priori*, that this assumption remains valid at substantially higher entrance speeds, especially in view of the imperfect gas and shock-wave boundary-layer-interaction effects already discussed.

The assumption of Prandtl number equal to unity would also appear permissible for the analysis of relative heating of missiles at the lower entrance speeds considered here. However, in view of the questionable effect (see again refs. 12 and 13) of dissociation on Prandtl number, it is not clear that this assumption is strictly valid at the intermediate and higher entrance speeds treated in this report.

From these considerations it is concluded that the simplifying assumptions made in the main heat-transfer analysis of this paper will not significantly influence the results at entrance speeds in the neighborhood of or less than 10,000 feet per second. However, at entrance speeds in the neighborhood of and greater than 20,000 feet per second, these results must be viewed with skepticism. More accurate calculations of heat transfer at these speeds must, among other things, await more accurate determinations of both the static and dynamic properties of air under these circumstances.

REFERENCES

1. Wagner, Carl: Skin Temperature of Missiles Entering The Atmosphere at Hypersonic Speed. Tech. Rep. No. 60, Ord. Res. & Dev. Division, Dept. of Army, Oct. 1949.
2. Dushman, Walter S.: Standard Atmosphere - Tables and Data. NACA Rep. No. 218, 1925.
3. Warfield, Calvin N.: Tentative Tables for the Properties of the Upper Atmosphere. NACA TN 1800, 1947.
4. Grünanger, G.: Probability that a Meteorite Will Hit or Penetrate a Body Situated in the Vicinity of the Earth. Jour. Appl. Phys., vol. 19, no. 10, Oct. 1948, pp. 947-956.
5. Sibulkin, M.: Heat Transfer Near the Forward Stagnation Point of a Body of Revolution. Jour. Aero. Sci., vol. 19, no. 8, Aug. 1952, pp. 570-571.
6. Mass. Inst. of Tech. Dept. of Elec. Engr., Center of Analysis: Tables of Supersonic Flow Around Cones, by the Staff of the Computing Section, Center of Analysis, under direction of Zdenek Kopal: Tech. Rep. No. 1, Cambridge, 1947.
7. Eggers, A. J. Jr., and Gavin, Raymond C.: Approximate Methods for Calculating the Flow About Nonlifting Bodies of Revolution at High Supersonic Airspeeds. NACA TN 2579, 1951.
8. Van Driest, E. R.: Turbulent Boundary Layer in Compressible Fluids. Jour. Aero. Sci., vol. 18, no. 3, Mar. 1951, pp. 143-146.
9. Van Driest, E. R.: Turbulent Boundary Layer on a Cone in a Supersonic Flow at Zero Angle of Attack. Jour. Aero. Sci., vol. 19, no. 1, Jan. 1952, pp. 55-57.
10. Richards, Elizabeth: Comparative Dispersion and Drag of Spheres and Right Cylinders. Aberdeen Proving Ground, Md., Ballistic Research Laboratories, Rep. T17, 1950.
11. Roedel, W. E.: Flow Separation Ahead of a Blunt Axially Symmetric Body at Mach Numbers 1.75 to 2.10. NACA TN 47129, 1951.
12. Moore, L. L.: A solution of the Laminar Boundary-Layer Equations for a Compressible Fluid with Variable Properties, Including Dissociation. Jour. Aero. Sci., vol. 19, no. 8, Aug. 1952, pp. 505-518.

13. Cross, J. Oored: The Laminar Boundary Layer at Hypersonic Speeds. NACA Rep. 2999, Apr. 13, 1952.
14. Lees, Lester, and Probstein, Ronald F.: Hypersonic Viscous Flow Over a Flat Plate. Princeton University Aeronomical Engineering Laboratory Rep. 195, Apr. 20, 1952.
15. Li, Ting-Ki, and Nagamatsu, Henry T.: Shock Wave Effects on the Laminar Skin Friction of an Insulated Flat plate at Hypersonic Speeds. GALCIT Memorandum No. 9, July 1, 1952.
16. Ruben, Morris W.: A Modified Reynolds Analogy for the Compressible Turbulent Boundary Layer on a Flat Plate. NACA TN 2317, 1953.

NACA TM 4047



NACA TM 4047

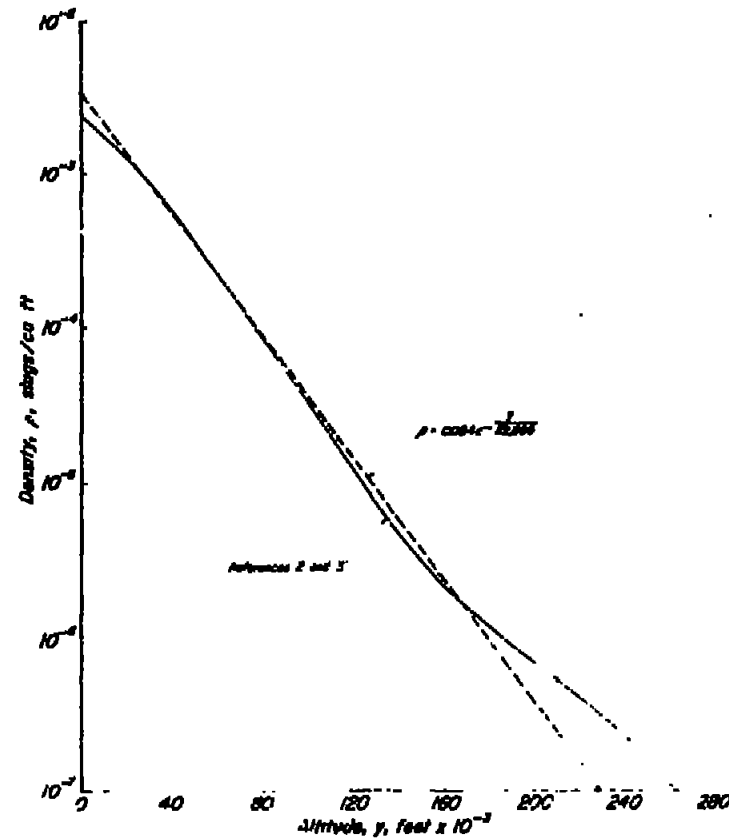


Figure - variation of density with altitude.

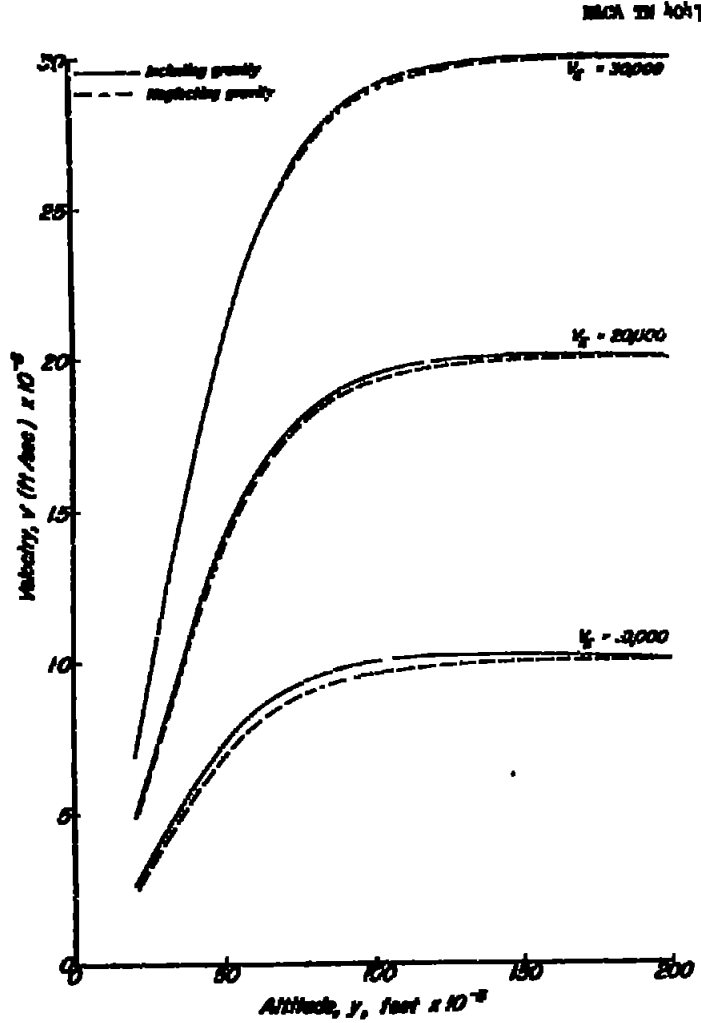


Figure 2.—Variations of velocity with altitude for a 1-foot diameter, solid iron sphere entering the earth's atmosphere vertically at velocities of 10,000, 20,000, and 30,000 ft/sec.

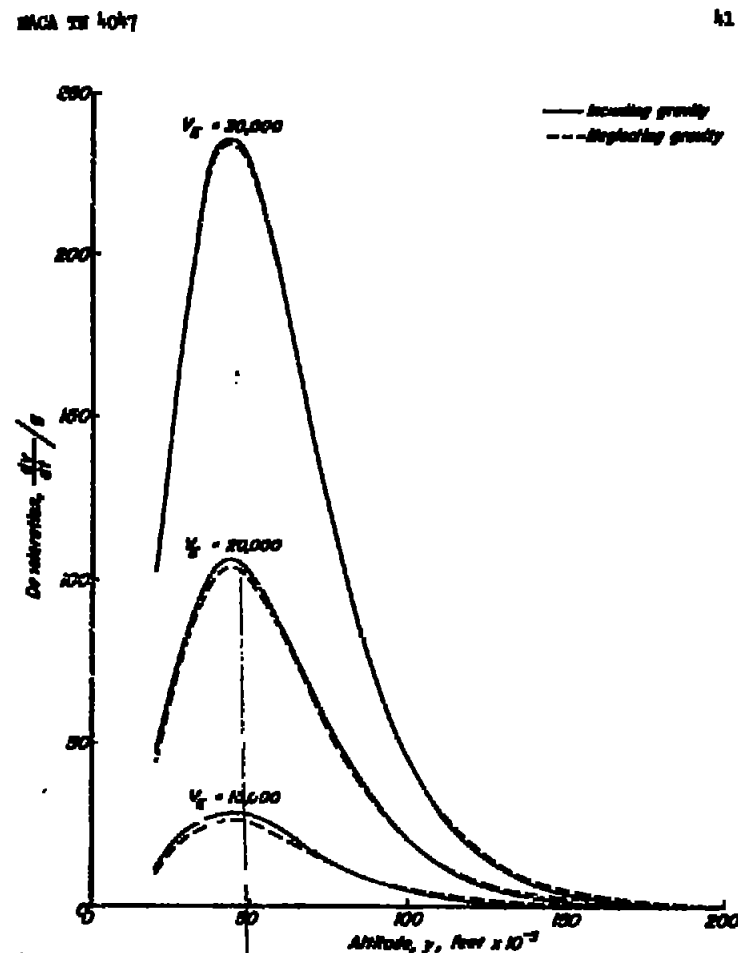


Figure 3.—Variations of deceleration with altitude for a 1-foot diameter, solid iron sphere entering the earth's atmosphere vertically at velocities of 10,000, 20,000, and 30,000 ft/sec.

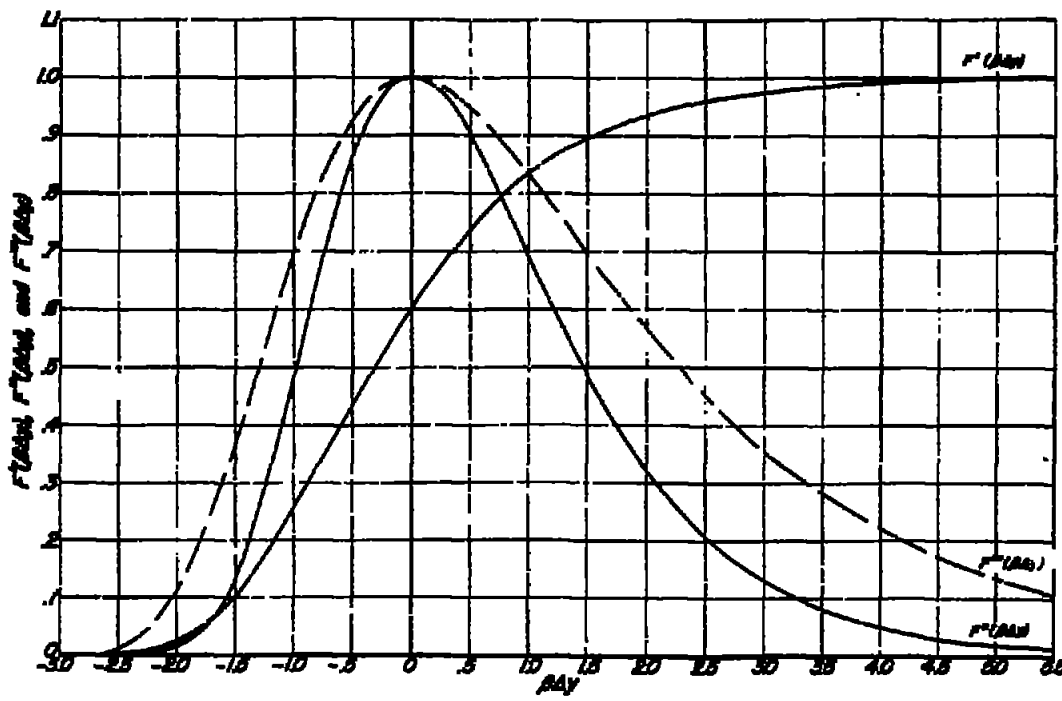


Figure 4—Variations of $F'(BDx)$, $F''(BDx)$, and $F'''(BDx)$ with BDx

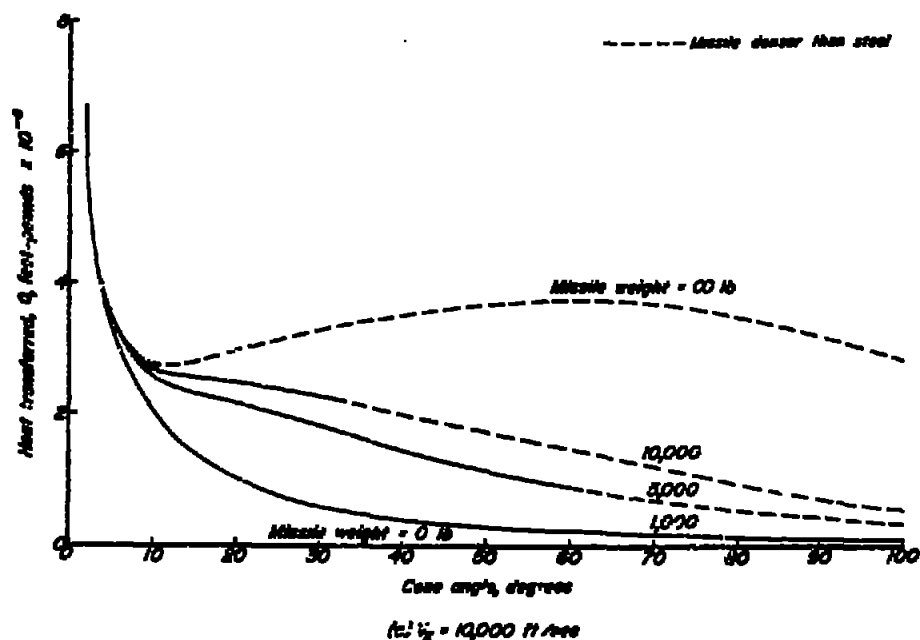


Figure 5—Convective heat transferred at impact to vertical missiles of some base area entering the earth's atmosphere at an angle of 30° to the horizontal and velocities of 10,000, 20,000 and 30,000 ft/sec (base area = 10 sq ft).

7-30-55 VEN

13

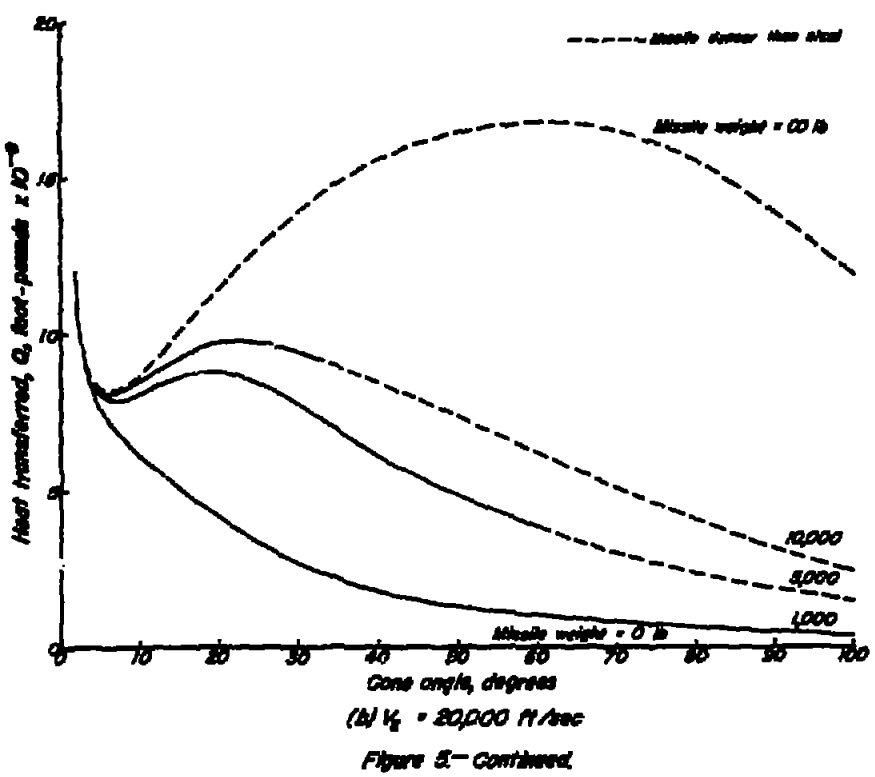


Figure 5—Continued.

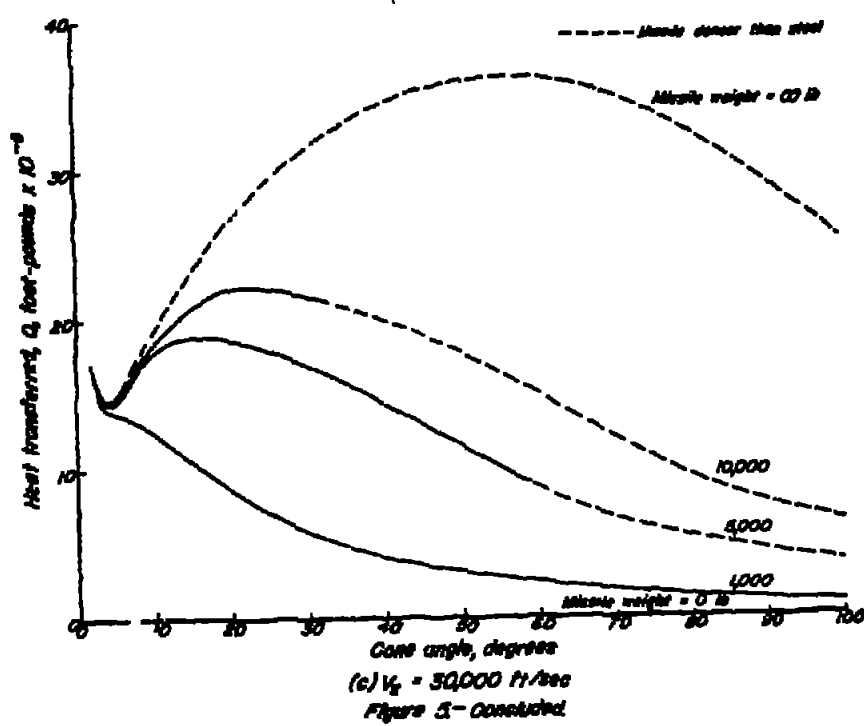


Figure 5—Continued.

5

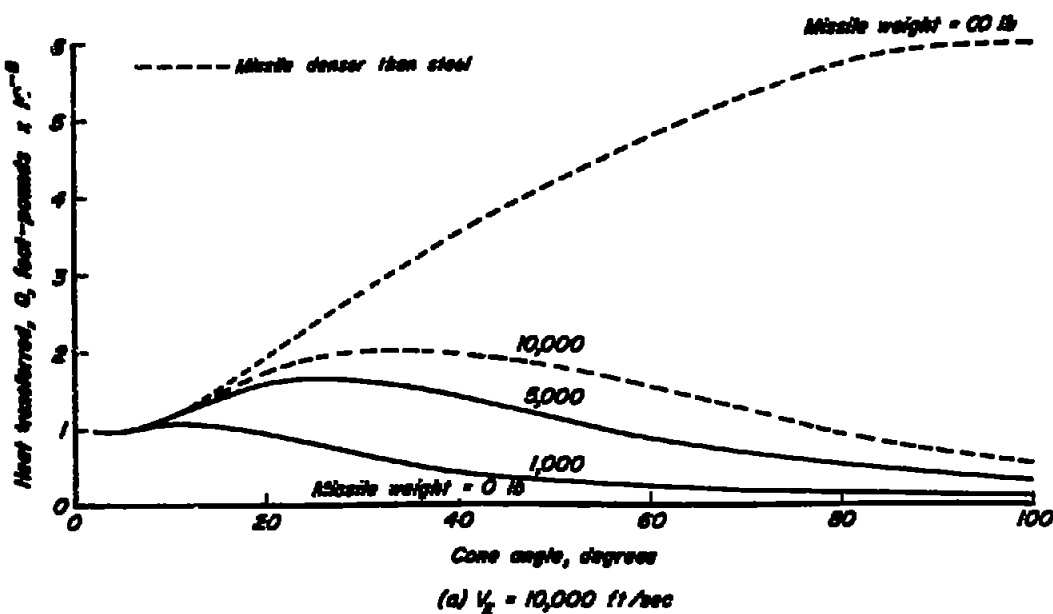


Figure 6.— Corrective heat transferred at impact to conical missiles of some volume entering the earth's atmosphere at an angle of 30° to the horizontal and velocities of 10,000, 20,000, and 30,000 ft/sec (volume = 16.34 cu ft).

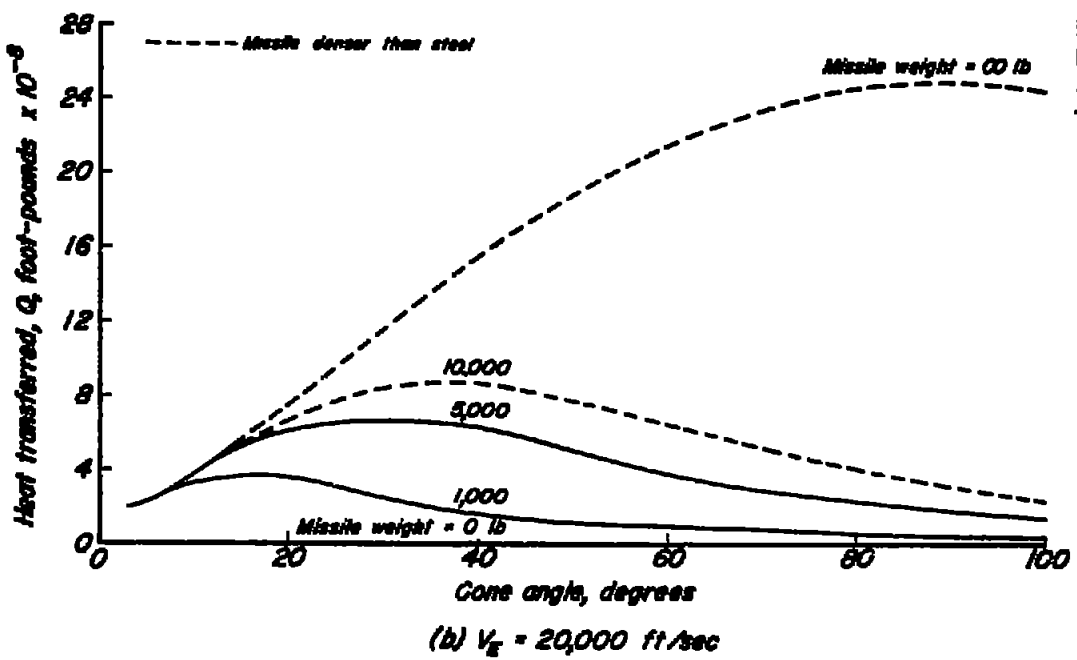


Figure 6.— Continued.

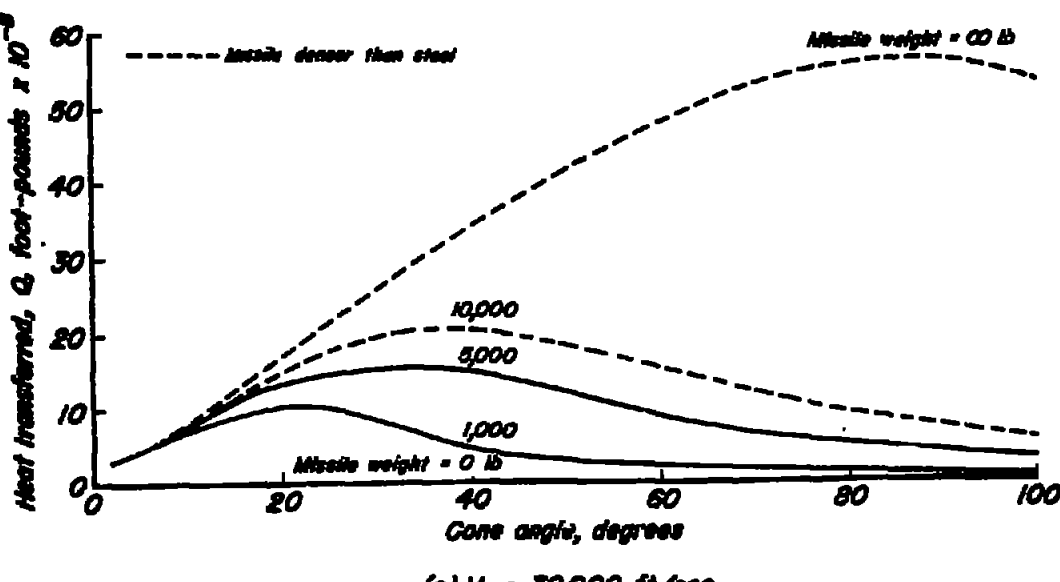
(c) $V_E = 30,000$ ft/sec

Figure 6.—Concluded.

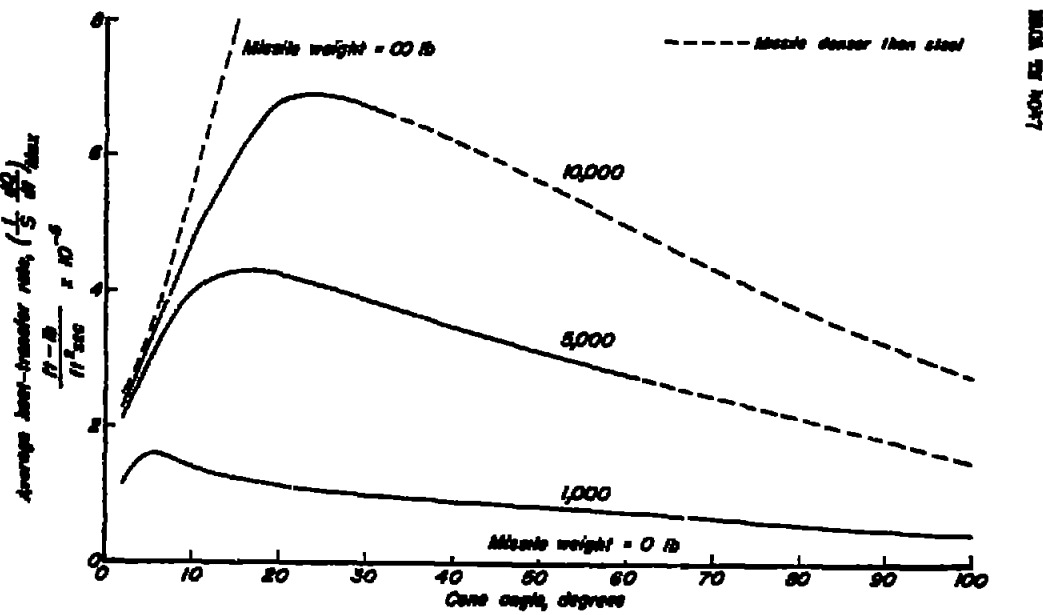
(a) $V_E = 10,000$ ft/sec

Figure 7.—Maximum average rate of convective heat transfer to conical missiles of the same base area entering the earth's atmosphere at an angle of 30° to the horizontal and velocities of 10,000, 20,000, and 30,000 ft/sec (base area = 10 sq ft).

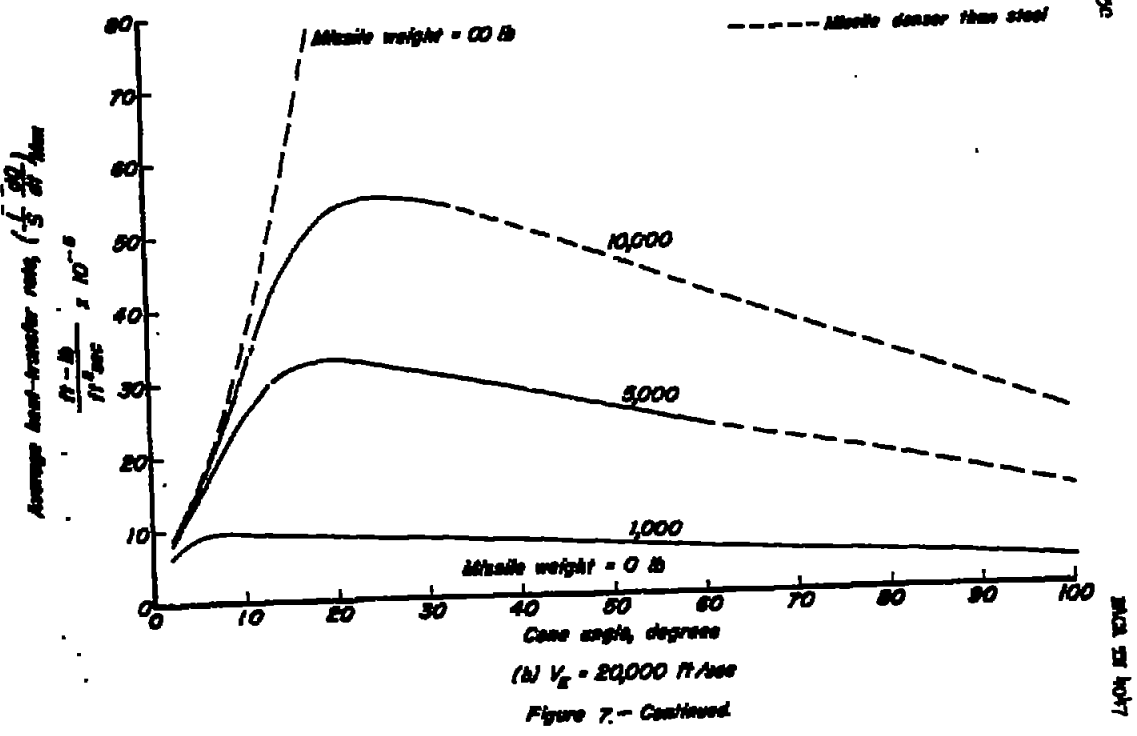


Figure 7 - Continued.

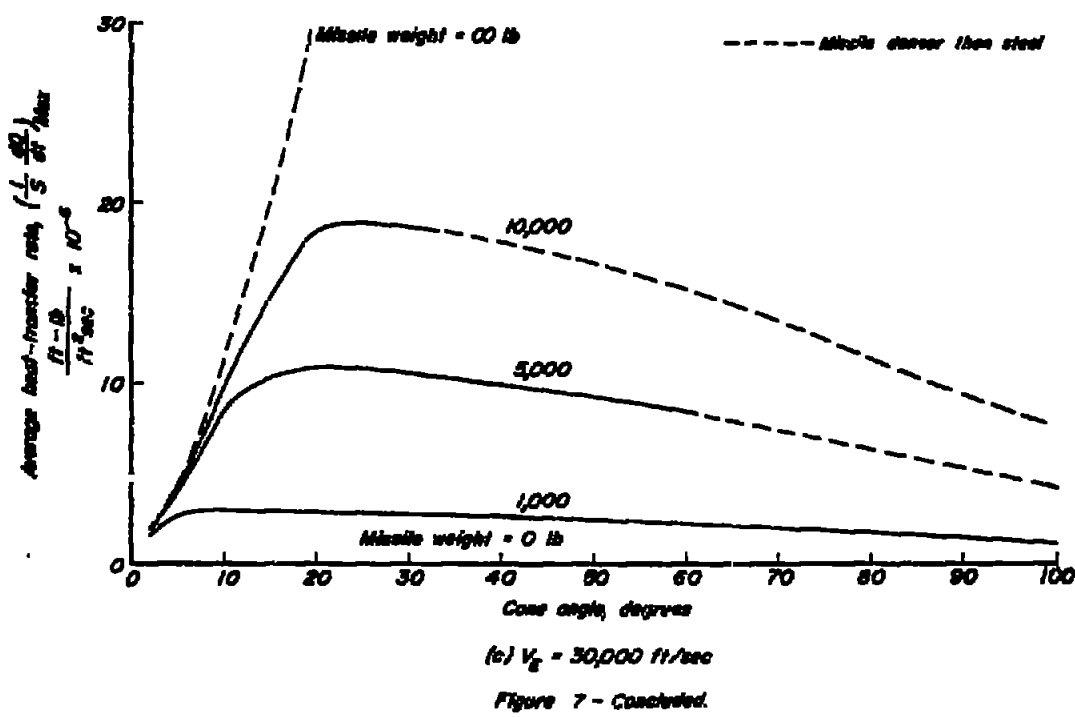


Figure 7 - Continued.

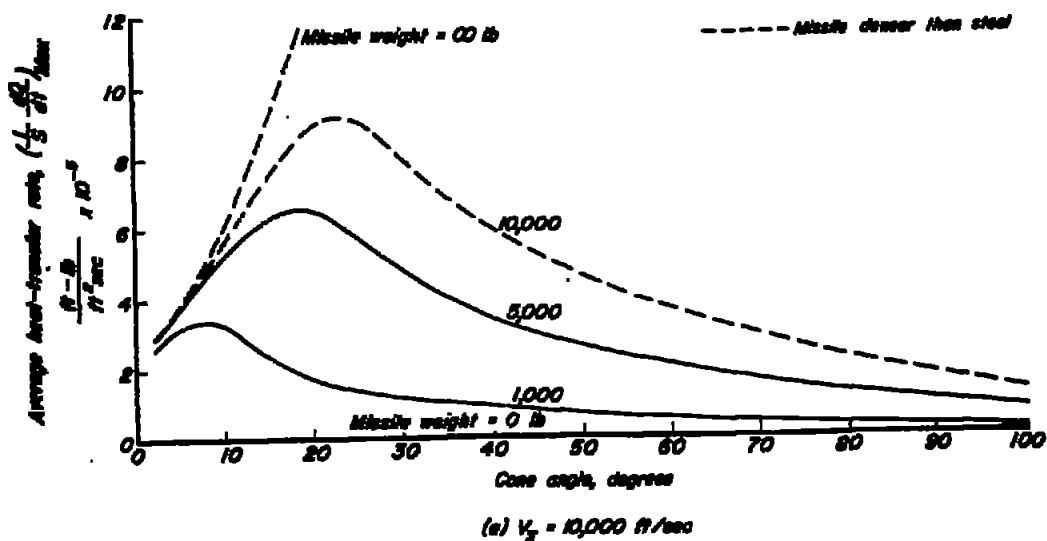


Figure 8.- Maximum average rate of convective heat transfer to conical missiles of the same volume entering the earth's atmosphere at an angle of 30° to the horizontal and velocities of 10,000, 20,000, and 30,000 ft/sec (volume = 16.34 cu ft).

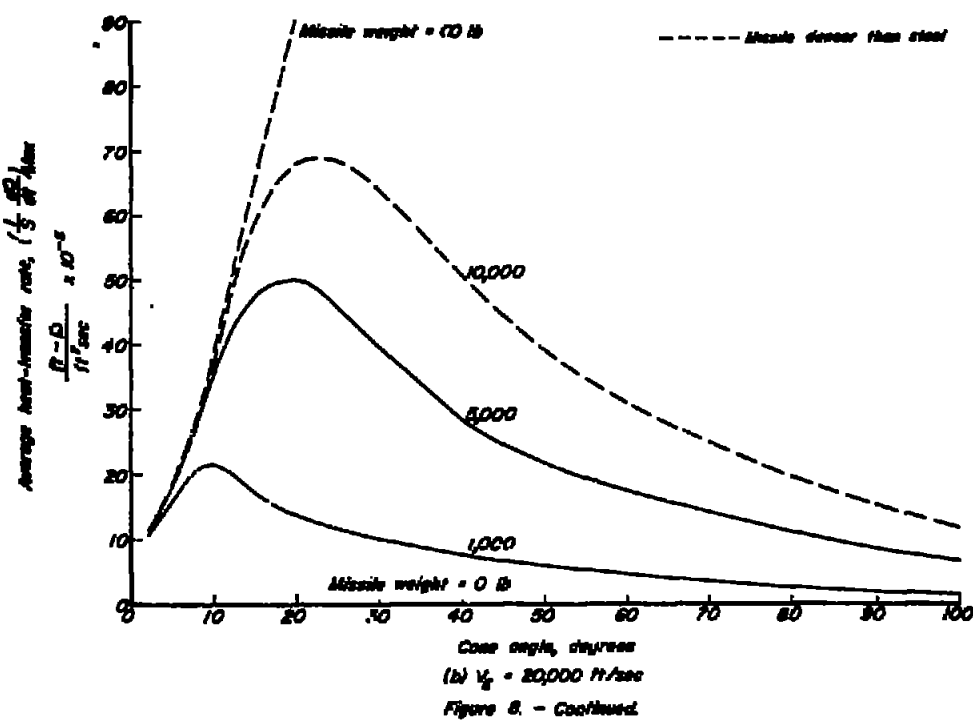


Figure 8. - Continued.

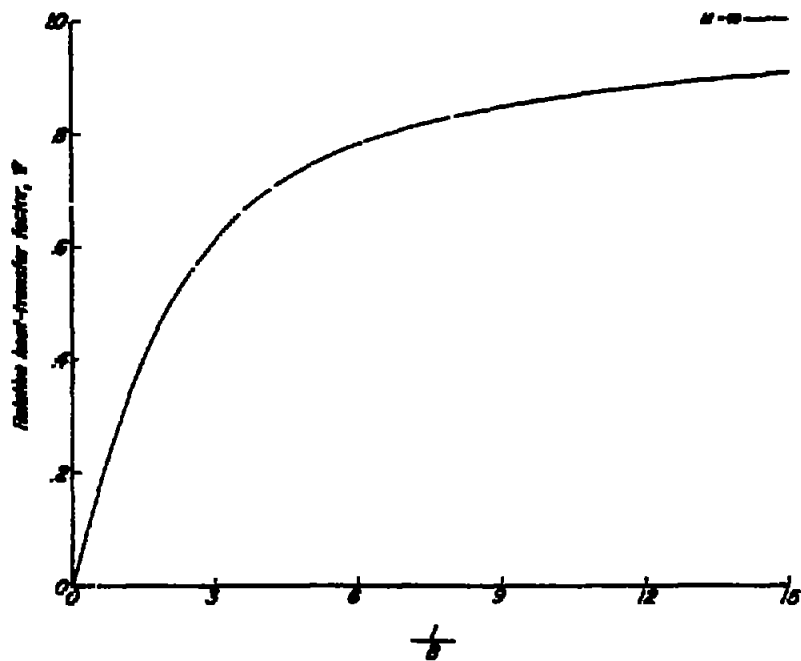
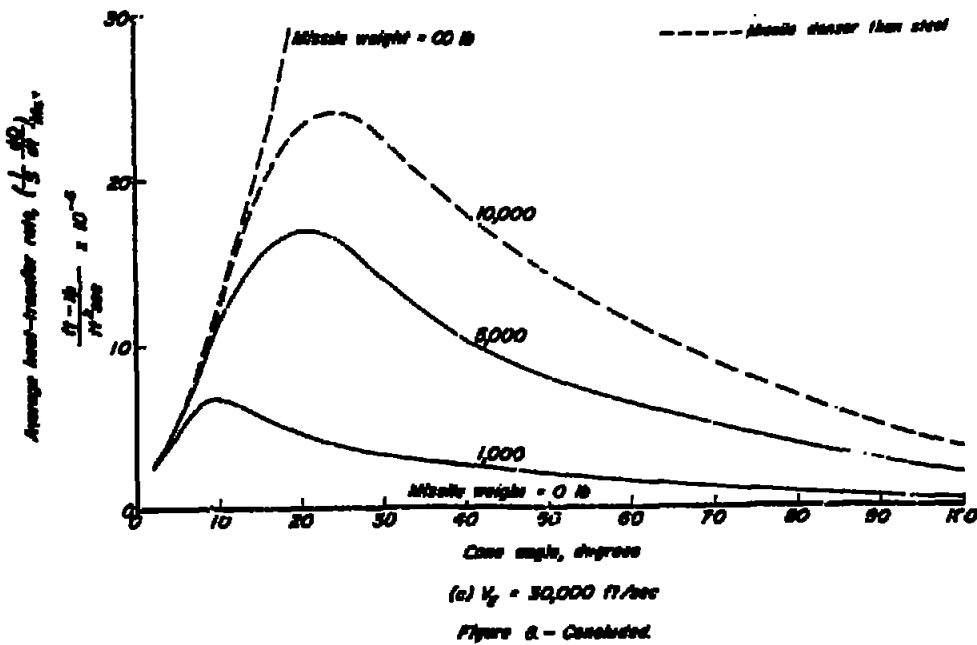


Figure 9 - Variation of relative heat-transfer factor F with $\frac{1}{B}$.

LORETTA
1977

LORETTA
1977

55

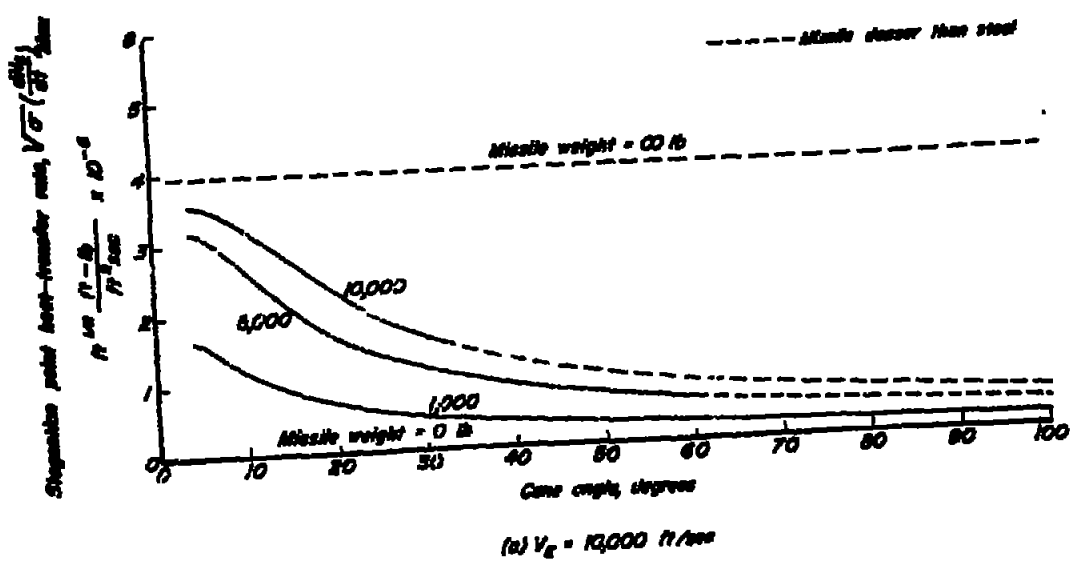


Figure 10.- Maximum rate of convective heat transfer to the stagnation point of spherically blunted cones of the same base area entering the earth's atmosphere at an angle of 30° to the horizontal and velocities of 10,000, 20,000, and 30,000 ft/sec (base area = 10 sq ft).

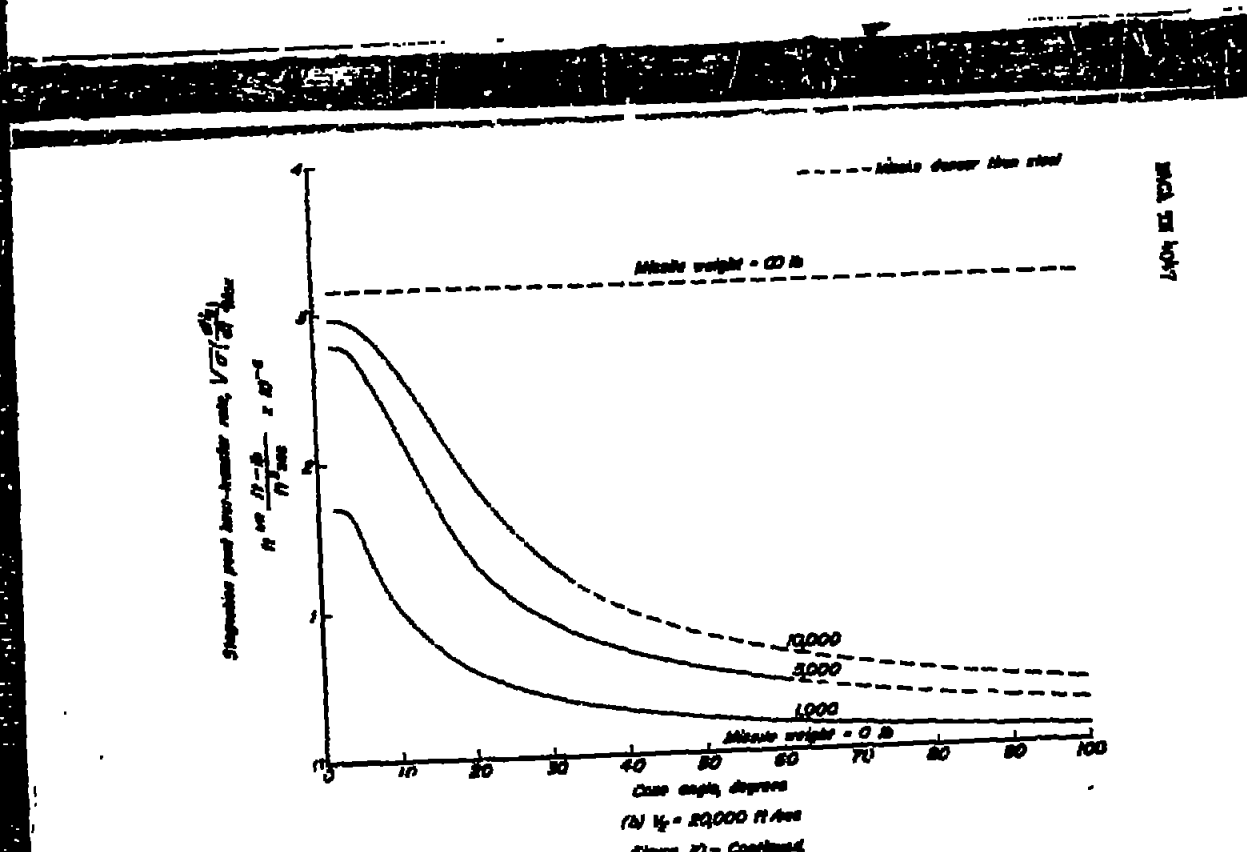


Figure 10—Continued

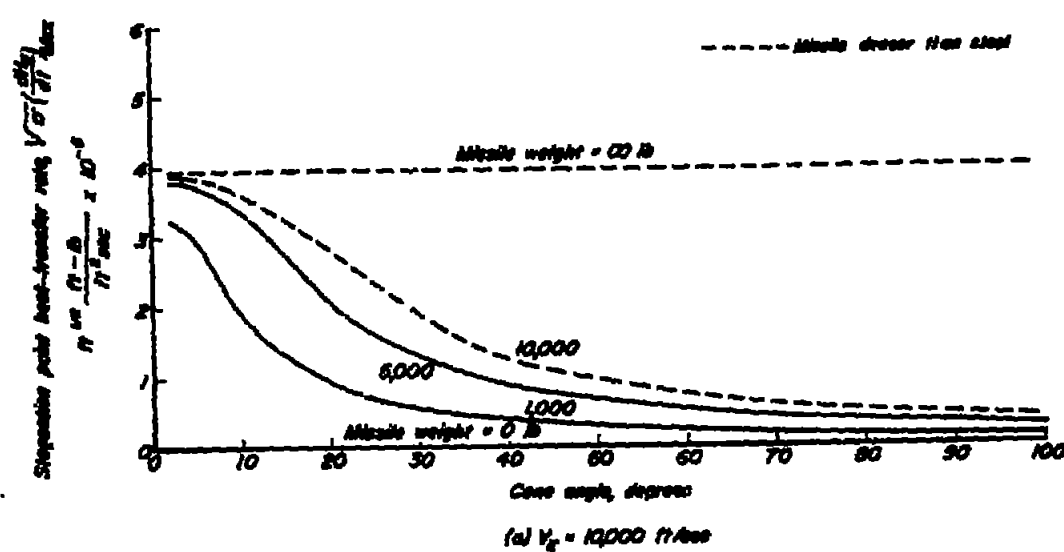
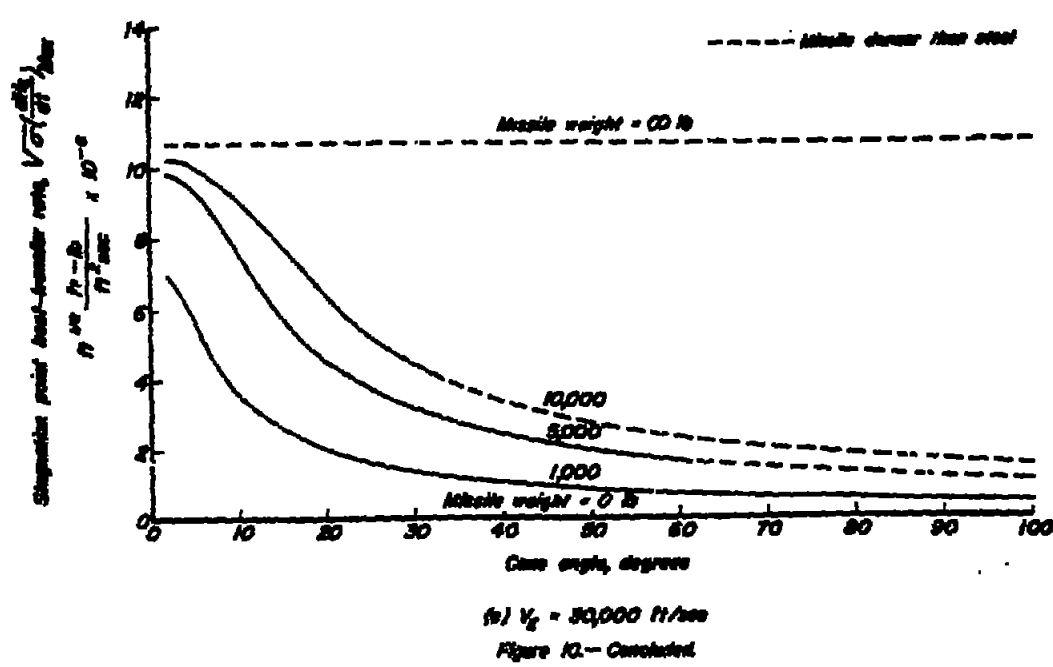


Figure 11.—Maximum rate of convective heat transfer to the stagnation point of spherically nosed cones of the same volume entering the earth's atmosphere at an angle of 30° to the horizontal and velocities of 10,000, 20,000, and 30,000 ft/sec (volume = 16.34 cu ft).

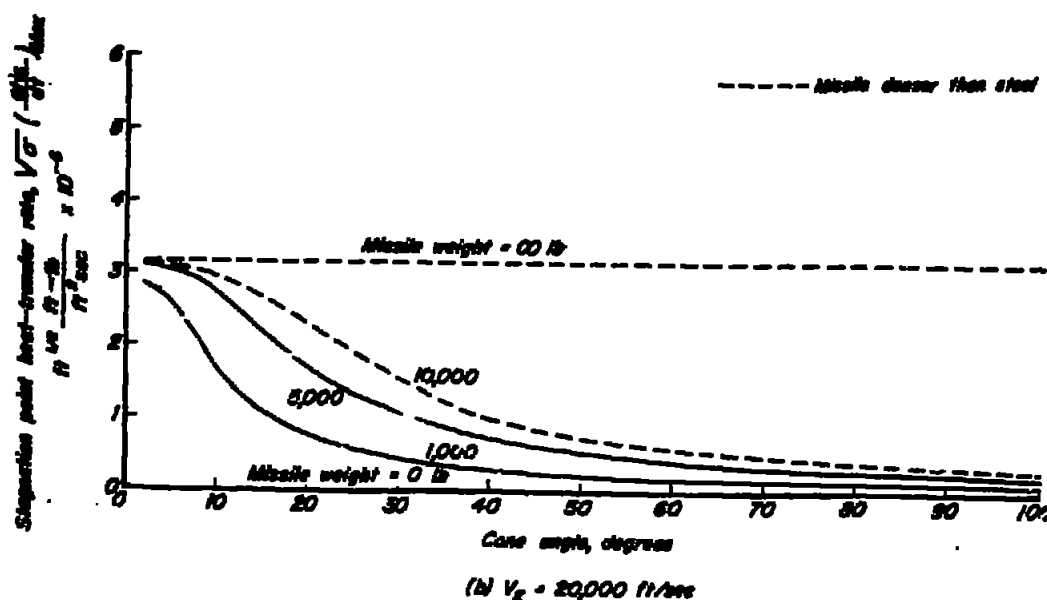


Figure 1L—Continued.

Liquor flow volume

Liquor flow volume

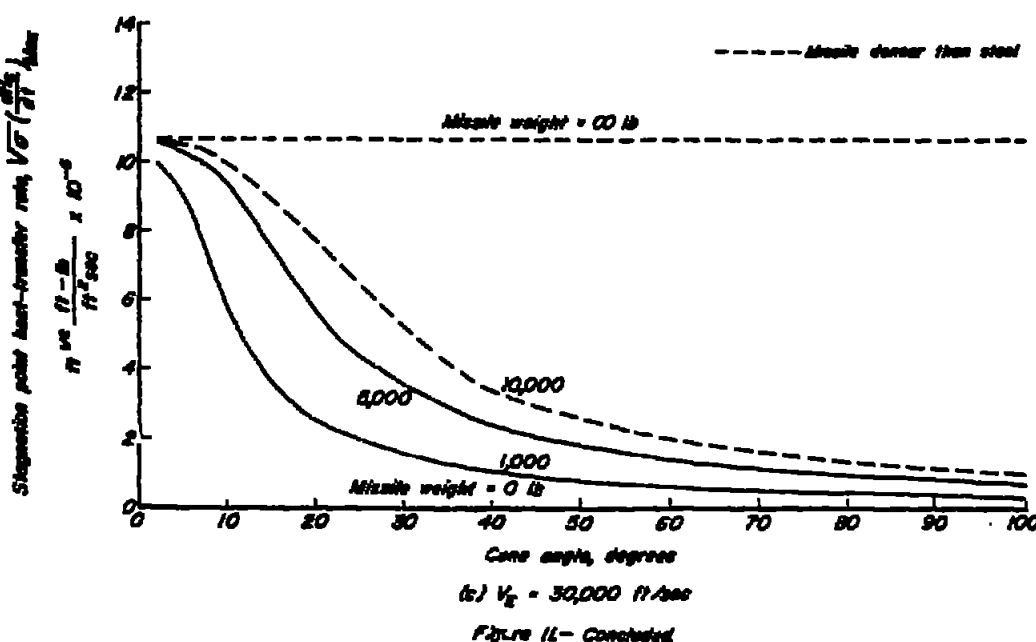


Figure 1L—Continued.

Liquor flow volume